DESIGN OF CENTRIFUGAL PUMPS

Feroz Ahmad

A Major Technical Report

in

The Faculty

of

Engineering

Presented in Partial Fulfillment of the Requirements
for the Degree of Master of Engineering at
Concordia University
Montreal, Quebec, Canada

April, 1979

ABSTRACT

DESIGN OF CENTRIFUGAL PUMPS

Feroz Ahmad

A practical approach to the design of centrifugal pumps is illustrated. The general features of centrifugal pumps are reviewed and a brief discussion of the design procedure is outlined. Equations necessary to determine the dimensions of the impeller and casing are presented. Empirical relationships based on experimental data are mentioned wherever available. The origin of the unbalanced forces developed in the pump casing is identified and methods to calculate the magnitude of such forces are given. Basic mechanical components of centrifugal pumps are summarised and a design example illustrating the approach and procedure outlined in this report is presented.

AKNOWLEDGEMENTS

The author wishes to express his appreciation to Dr. G.D. Xistris for the invaluable suggestions, encouragement and time spent by him throughout the course of this report.

The author also wishes to thank Miss Clotilde Leone for typing this report.

TABLE OF CONTENTS

LIST OF FIGURES

LIST OF TABLES

NOMENCLATURE

Symbol	Description	Units
A_{th}	Throat velocity	in^2 (mm^2)
A_v	Volute area	in^2 (mm^2)
BHP	Brake horsepower	hp (KW)
B_2	Outlet width of impeller including shrouds	in (mm)
C	Dynamic capacity of bearing	lbs (Kg)
C_o	Static capacity of bearing	lbs (Kg)
D_e	Eye diameter	in (mm)
D_s	Shaft diameter	in (mm)
D_H	Hub diameter	in (mm)
E	Modulus of Elasticity	psi (N/mm^2)
F_a	Axial thrust	lbs (Kg)
F_r	Radial thrust	lbs (Kg)
F_1	Radial load on inboard bearing	lbs (Kg)
F_2	Radial load on outboard bearing	lbs (Kg)
H	Head at design point	ft (m)
H_o	Head at zero flow	ft (m)
I	Moment of Inertia	in^4 (mm^4)
K_r	Radial thrust coefficient	
M	Bending moment	lb-in (Kg.mm)
N	Rotative speed	r.p.m.
N_c	Critical speed	r.p.m.
P	Equivalent bearing load	lbs (Kg)

Q	Flow	USGM (m^3/s)
Q_L	Leakage flow	USGM (m^3/s)
R_2	Impeller outlet radius	in (mm)
R_t	Tongue radius	in (mm)
R_e	Eye radius	in (mm)
S_s	Shear stress	psi (N/mm^2)
SG	Specific gravity	
T	Torque	lb-in (N.mm)
V	Rotation factor of bearing	
W	Load	lbs (Kg)
X	Radial factor of bearing	
Y	Thrust factor of bearing	
Z	Number of vanes	
a	Constant coefficient of volute	
b_1	Inlet width	in (mm)
b_2	Outlet width	in (mm)
b_3	Volute width	in (mm)
c_1	Inlet absolute velocity	ft/sec (m/s)
c_2	Outlet absolute velocity	ft/sec (m/s)
c_{m_1}	Inlet meridional velocity	ft/sec (m/s)
c_{m_2}	Outlet meridional velocity	ft/sec (m/s)
c_{u_1}	Peripheral component of inlet absolute velocity	ft/sec (m/s)
c_{u_2}	Peripheral component of outlet absolute velocity	ft/sec (m/s)
g	Acceleration due to gravity	ft/sec^2 (m/s^2)
h	Volute height	in (mm)

l	Length	in (mm)
p	Pressure	psi (N/mm^2)
t	Thickness of vanes	in (mm)
u	Peripheral velocity	ft/sec (m/s)
v_e	Eye velocity	ft/sec (m/s)
w	Relative velocity	ft/sec (m/s)
y	Deflection	in (mm)
α_1	Inlet flow angle	degrees
α_2	Outlet flow angle	degrees
α_3	Angle of diffusion	degrees
β_1	Inlet vane angle	degrees
β_2	Outlet vane angle	degrees
γ	Density	lb_m/ft^3 (Kg/m^3)
ε_1	Inlet contraction factor	
ε_2	Outlet contraction factor	
ϕ_v	Volute angle	degrees
ϕ_t	Tongue angle	degrees
$\bar{\phi}$	Angle	radians
ℓ	Radius of arc	in (mm)
η	Overall efficiency	per cent
η_v	Volumetric efficiency	per cent
η_H	Hydraulic efficiency	per cent
ψ	Head coefficient	
μ	Slip factor	

CHAPTER 1

INTRODUCTION

CHAPTER I

INTRODUCTION

1.1 Principal Features of Centrifugal Pumps

Simplicity, economy and reliability are the primary reasons why centrifugal pumps are selected for most liquid transfer applications involving low to moderate heads and viscosities less than 1,000 centipoise.

In these pumps, the liquid enters the impeller at the centre and is flung outwards under the action of centrifugal forces set up by the rotation of the impeller. The impeller action causes an increase in the liquid velocity and pressure. The imparted velocity is partly converted into pressure by the pump casing before it leaves the pump through the discharge nozzle. This conversion may be accomplished either in a volute casing or in a diffuser casing.

In a volute casing, the impeller discharges into a channel of gradually increasing area designated as the volute. This arrangement is illsutrated in Figure 1.1. The major part of the velocity conversion in volute casings, takes place in the conical discharge nozzle section. Figure 1.2 shows a typical diffuser casing. In such a design, the impeller discharges into a channel provided with vanes. The contour of the vanes determines to a large extent the degree of velocity to pressure transformation achieved in a given design.

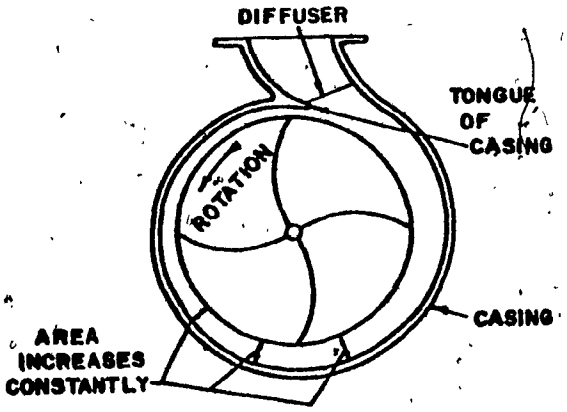

Figure 1.1 - Typical Volute-Type Pump

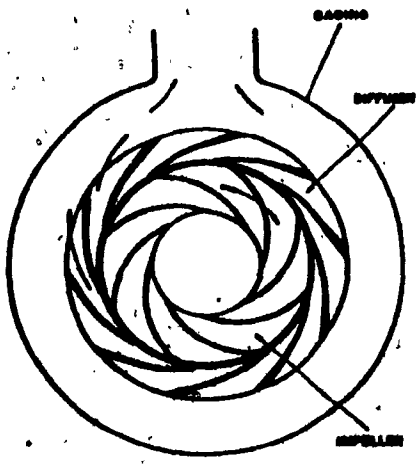

Figure 1.2 - Typical Diffuser-Type Pump

1.2 Performance Variables

The performance of a centrifugal pump is generally measured in terms of the following parameters:

Rate of flow or capacity (Q) measured in gallons per minute (metre^3/sec), increase of energy level in the liquid pumped or head (H) measured in feet (metre), input power (P) expressed as brake horsepower in HP (KW), efficiency (η) defined as the ratio of useful work performed to power input and lastly, rotating speed (N) expressed in rpm. Since these parameters are mutually interdependent, it is customary to represent the performance of a centrifugal pump by means of characteristic curves for each generic type. Figure 1.3 is such a typical curve depicting the Head-Capacity (H-Q), BHP-Capacity and the Efficiency-Capacity for a particular model of a volute casing centrifugal pump.

1.3 Operational and Design Considerations

The most important operating characteristics are the capacity, head, power and efficiency. It is customary to plot the head, power and efficiency as functions of capacity for a given operating speed. Pumps are selected to operate at the maximum efficiency point. The head, power and capacity which correspond to the maximum efficiency point are designated as the normal values and are denoted as Q_n, H_n and P_n respectively. At times, a pump may be operated continuously at a capacity slightly above or below the best efficiency point. In these cases the actual operating point is called the rated or guaranteed point.

It should be pointed out that a variety of operating requirements can be met from the same pump model by changing the outside diameter of

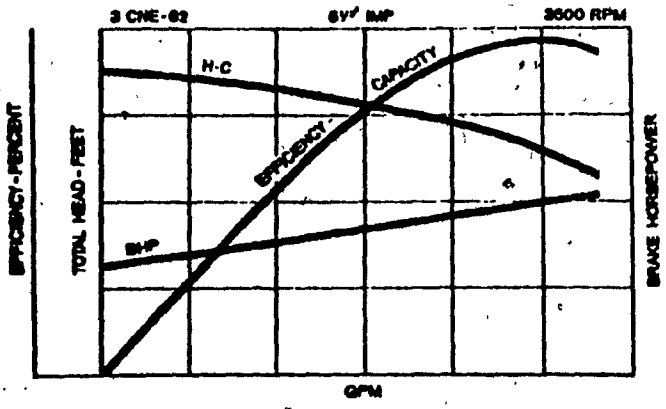

Figure 1.3 - Characteristic Curve

the impeller. The principal requirement in the design of centrifugal pumps is the determination of the impeller and casing dimensions which will produce the specified conditions of capacity and head. In the following sections, the parameters and equations governing the design of volute type centrifugal pumps (impeller, casing, radial and axial thrust, etc.) will be developed. Current industrial practice will be illsutrated by means of an actual design example for a typical volute type centrifugal pump application.

1.4 Procedure for the Design of Centrifugal Pump

1.4.1 Design Criteria

The basic purpose of a centrifugal pump is to add energy to the fluid. Since this is a dynamic process, the pump depends entirely on changes in the velocity relationships to achieve the required changes in the energy level. Changes in the energy level of the fluid are detected largely through measurements of static pressure.

Many investigators have attempted to develop improved centrifugal pump design methods through analytical calculations of two- and three-dimensional velocity distributions within the fluid passages [1]. However, it has been shown that the most useful application of internal-velocity calculations is limited to the analysis of a large number of impeller/casing combinations for high and low efficiency. This semi-empirical approach is the most likely to identify optimum velocity schedules which can be used for new designs.

The actual velocity relationships existing within a centrifugal pump are extremely complex and to a substantial degree remain unknown.

For most practical purposes, a one-dimensional analysis is adequate to illustrate the basic concepts and indeed has served as the basis of design for virtually all centrifugal pumps manufactured to date.

1.4.2 Design Data

Considerable use of published experimental data is made in pump design work. These data are normalized in terms of the specific speed parameter which is defined as [2]:

$$N_s \triangleq \frac{N\sqrt{Q}}{H^{3/4}} \tag{1.1}$$

where N_s is specific speed, N is revolutions per minute, Q is flow in gallons per minute (metre^3/sec) and H is head measured in feet (metre).

For a pump with a specific speed N_s, with an impeller of diameter D, pumping Q gallons per minute at a speed of N rpm against a head of H feet, the specific speed N_s is equal to the speed of a geometrically similar pump with an impeller of diameter d which would have a discharge of one gallon per minute against a head of one foot.

This correlation is based on the premise that geometrically similar pumps, operated at the same specific speed have geometrically similar velocity triangles. Consequently, the ratio of the flow velocity to the impeller peripheral speed is the same for geometrically similar units and were it not for the scale effects, their relative losses would be the same.

The specific speed is always based on the optimum operating conditions or peak point of pump performance. Figure 1.4 is typical illustra-

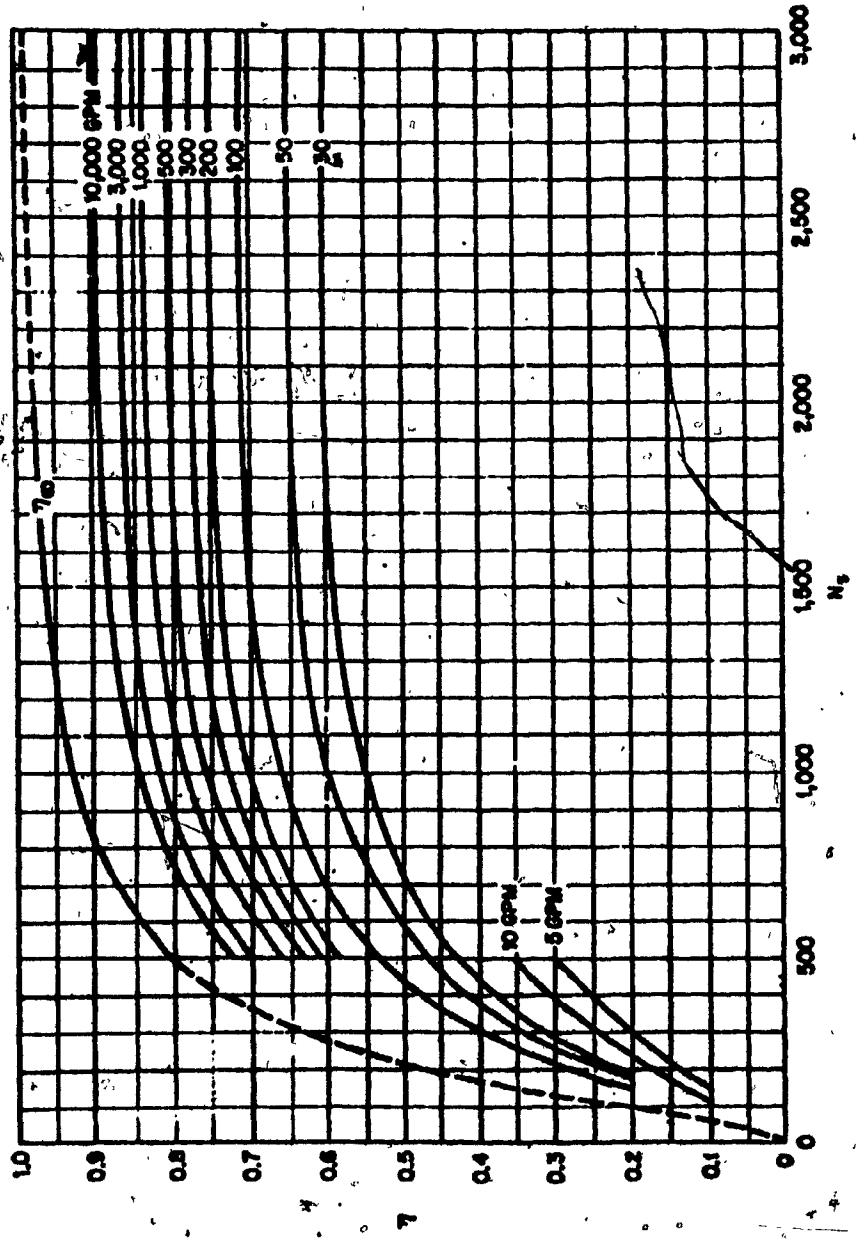

Figure 1.4 - Efficiency as a Function of Specific Speed and Capacity [3]

tion of performance data presented in terms of specific speed, where efficiency n is plotted versus specific speed N_s with Q as a parameter. Knowing the head and capacity which are normally derived directly from the desired service conditions, the efficiency may be found for any pump rpm from Equation 1.1. Similiar correlations involving other pump operting parameters have been developed and these will be illustrated in later sections of the report.

CHAPTER 2

IMPELLER DESIGN

CHAPTER 2

IMPELLER DESIGN

2.1 Introduction

In centrifugal pumps, fluid movement is achieved by increasing the level of pressure energy (head) utilizing an impeller with appropriately shaped blades. The particles of liquid in the impeller passages are accelerated from the suction towards the delivery side of the pump as a result of the impeller rotation. The amount of pressure energy imparted to the fluid depends on the velocity developed by the impeller and the characteristics of the casing.

The performance of a given pump design is determined by plotting the head, power and efficiency as a function of capacity at a constant speed. This is a function of the geometrical dimensions and speed for a specific pump. Analytical investigations of fluid movement in an impeller are usually limited to axi-symmetric flow models. This analysis is valid for impellers with a large number of vanes of infinitesimal thickness and consequently, modification must be introduced before extending these results to the design of actual impellers. In order to achieve correct results, it is necessary to distinguish between idealised and real velocities. This is accomplished by introducing a number of design factors such as slip and prerotation.

For axi-symmetric flows, the flow characteristics depend on the radius and the axial co-ordinate measured along the axis of symmetry. Thus, the absolute (referred to the stationary pump casing) and relative

(referred to the impeller) velocities are functions of the co-ordinates 'r' and 'z' alone and do not depend on the angle θ.

Referring to Figure 2.1, it can be seen that the absolute velocity c can be resolved into two flow components: meridional flow in which the liquid particles move with velocity c_m in planes passing through the impeller axis, and circumferential flow, in which the liquid particles move with velocity c_u on circles centered on the impeller axisand lying in planes perpendicular to it.

2.1.1 Velocity Components

Figure 2.1 represents the inlet and outlet ideal velocity triangles, where u is the peripheral velocity of any point on a vane and w is the velocity of a fluid particle relative to the impeller. The absolute velocity c of a fluid particle is the vector sum of u and w. The absolute velocity vector c may be resolved into meridional or radial velocity c_m and peripheral velocity c_u. The subscripts 1 and 2 refer to the inlet and outlet cross-section of the flow passages.

2.1.2 Angles

Figure 2.1 indicates the angles between different velocity vectors. α_1 is the angle at which flow enters the impeller and α_2 is the angle at which flow leaves the impeller. Angles β_1 and β_2 are the inlet and outlet vane angles and β is the angle made by a tangent to the impeller vane and a line in the direction of motion of the vane. Angles β_1 and β_2 define the vane curvature and establish the vane geometry. α_2 gives the direction with which the fluid enters the casing and it also establishes

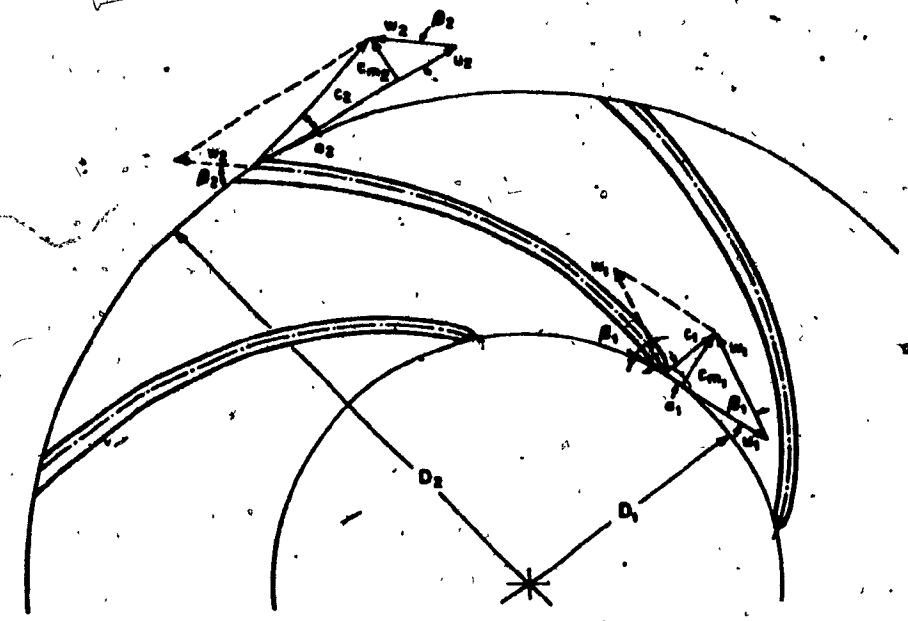

(A)

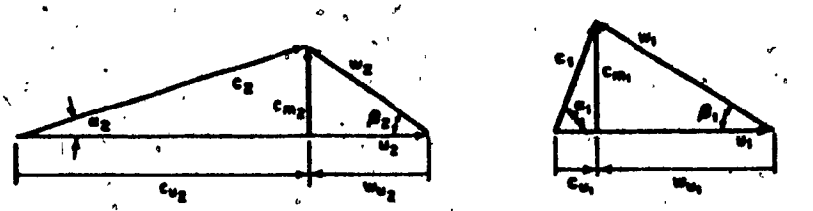

EXIT VELOCITY TRIANGLE

ENTRANCE VELOCITY TRIANGLE

(B)

Figure 2.1 – Velocity Diagrams for Radial-Flow Impellers

the casing tongue angle.

2.1.3 Prerotation of Fluid

For design purposes, it is assumed that the flow enters the impeller at an angle α_1 equal to 90° and that the peripheral component of the absolute velocity c_{u_1} is zero. This implies that there is no prerotation of the fluid before entering the blades. In real cases, this is not true and experimentally, it has been confirmed that there is a discrepancy between the flow calculated on the above assumption and the measured flow. This suggests that there is prerotation of fluid before entry into the vanes even at the best efficiency point. In order to attain the required discharge Q_n, it is found necessary to increase the blade angle β_1 by an appropriate amount. The inlet velocity triangle, taking into account the above, can be represented as shown in Figure 2.2.

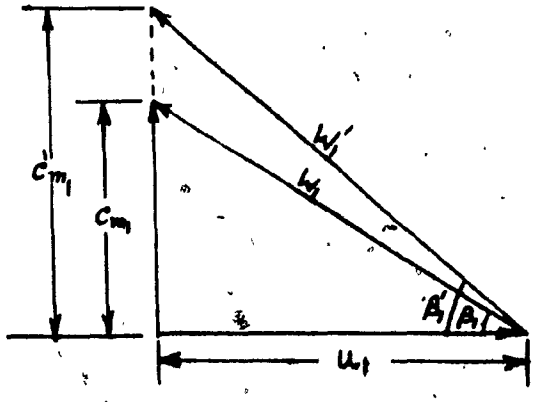

Figure 2.2 - Inlet Velocity Triangle Without Prerotation

2.1.4 Slip

The ideal case is based on the assumption of an infinite number of vanes having infinitesimal thickness. But in reality, the impeller has a finite number of blades having finite thickness. This alters the flow pattern within the impeller passages formed by the impeller vanes and

the shrouds. Due to the rotation of the impeller, there will be a through-flow or meridional flow through the passages and also a forced vortex set-up within the passages due to the inertia of the liquid tending to rotate in the opposite direction relative to the impeller. The resultant effect for a given flow is to cause the fluid to leave the impeller at an angle less than the vane angle β_2, at which the fluid leaves the impeller. Figure 2.3 shows the velocity distribution in the impeller passages of a centrifugal pump taking into account the influence of the forced vortex of the liquid in the passages. This phenomenon is often called slip.

From figure 2.3, it will be seen that the actual peripheral component of absolute velocity is c'_{u_2} and not c_{u_2} as assumed in the ideal case. This velocity deviation causes a reduction in the total head of the liquid. So the ideal peripheral component of absolute velocity c_{u_2} has to be corrected in order to arrive at the design head. Since the actual velocity distribution over the discharge cross-section is not known, it is impossible to determine the true effective value of c_{u_2} analytically. For practical calculations, an empirical coefficient called slip factor μ has been developed to account for the actual flow deviations. The slip factor is defined as:

$$\mu = \frac{c'_{u_2}}{c_{u_2}} \qquad (2.1)$$

2.2 Impeller Dimensions

The standard centrifugal pump can be divided into three sections. The inlet section which is characterised by the shaft diameter, hub

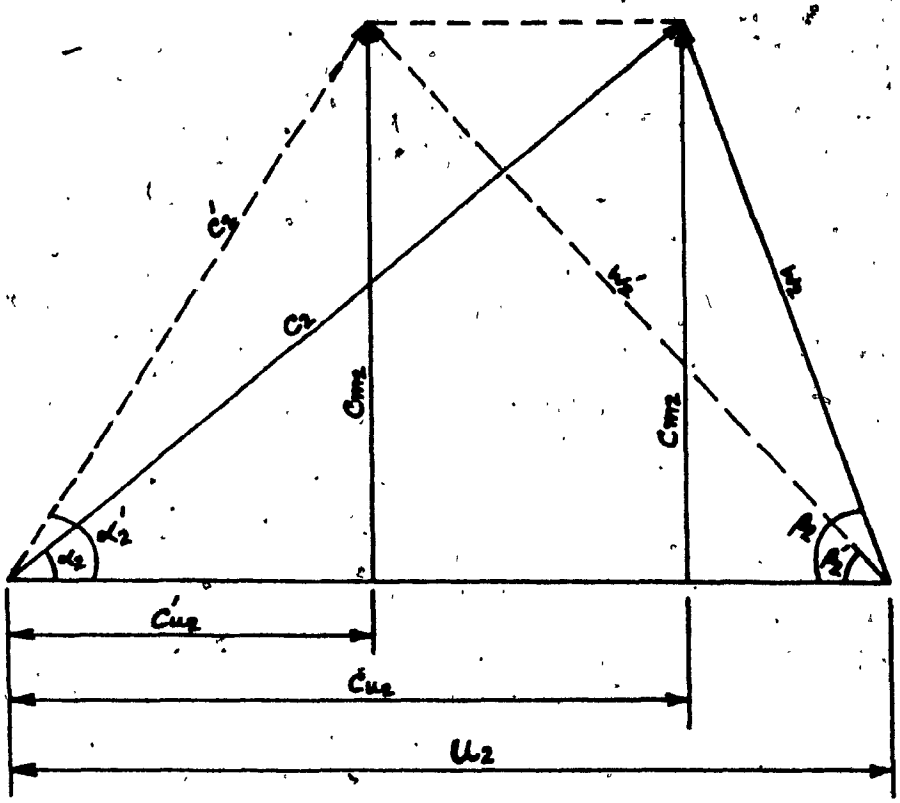

Figure 2.3 - Outlet Velocity Triangle

Taking into Account the Slip

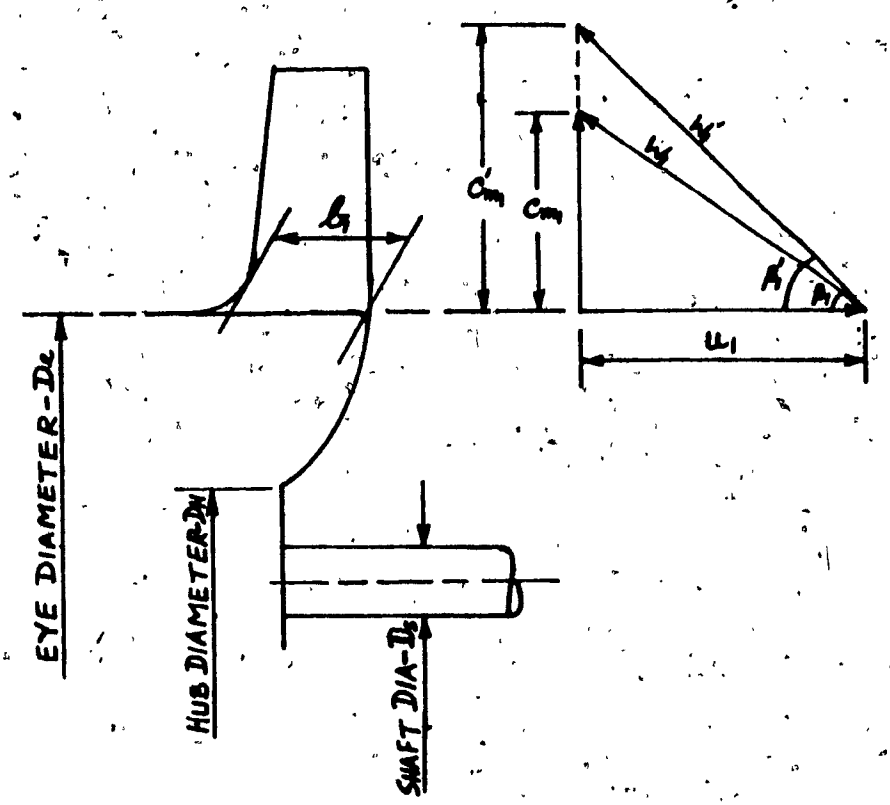

Figure 2.4 - Typical Inlet Section With Corresponding Inlet Velocity Triangle

diameter, impeller eye diameter, inlet vane angle and the inlet width. The outlet section is specified by the impeller outlet diameter and the outlet width. The third section encompasses the impeller vanes and this is described by defining the vane curvature.

2.2.1 Inlet Section

The design of the inlet section involves the specification of the shaft diameter, hub diameter, impeller eye diameter, inlet angle and inlet width. A typical inlet section configuration is illustrated in Figure 2.4, along with the corresponding inlet velocity diagram.

The shaft diameter is determined by considering the power to be transmitted, the critical speed and the maximum permissible deflection for the given mode of operation. Initially, the shaft diameter is estimated on the basis of torque requirements alone [4]. The torque may be found from:

$$T = \frac{63000 \times BHP}{N} \tag{2.2}$$

or:

$$T = \frac{9.55 \times 10^6 \times BHP}{N} \tag{2.2A}$$

where T is the torque measured in lb-in (Newton-mm), BHP is the brake horsepower, as defined below, measured in HP (KW) and N is the revolutions per minute.

Brake horsepower is defined by

$$BHP = \frac{Q \times H \times SG}{3960 \times \eta} \tag{2.3}$$

or

$$BHP = \frac{\gamma \times g \times Q \times H}{1000} \qquad (2.3A)$$

where Q is the flow measured in gallons per minute (m^3/sec), H is the head measured in feet (metre), η is the overall efficiency, S.G. is the specific gravity, γ is the density in Kg/m^3 and g is the acceleration due to gravity. It should be noted that all the terms appearing on the right-hand side of equation (2.3) are either given or obtainable from Figure 1.5. Finally, the shaft diameter, based on shear stress considerations alone, may be found from:

$$D_s = \left[\frac{5.1T}{S_s}\right]^{1/3} \qquad (2.4)$$

where D_s is the shaft diameter in inches (mm), T is the torque measured in lb-in (N.mm) and S_s is the allowable shear stress in psi (N/mm^2) for a given material. The shaft diameter, as calculated from Equation 2.4, must be increased to account for the presence of bending moments arising from the impeller reaction and the shaft mass. The impeller bending moments are caused by unbalance forces and the net radial thrust developed. If these quantities are known, the exact correction to the diameter may be calculated. However, initially an arbitrary increase based on past experience is used, and once the critical speed analysis of the shaft has been completed, these dimensions are adjusted accordingly. At this stage, it is not possible to determine the weight of the impeller and the correpsonding radial thrust since the overall dimensions of the impeller are still unknown.

Good design practice requires that the hub diameter on the inlet side be made as small as practical so that the inflow into the impeller

eye encounters the least resistance possible. This condition is attained by choosing a hub diameter which is 30% - 40% greater than the shaft diameter. In cases where the impeller hub does not extend into the eye, the hub diameter can be taken as zero.

The inlet eye diameter can be calculated using the continuity equation [5]:

$$D_e = \left[\frac{1.28Q}{\pi \eta_v V_e} + D_H^2\right]^{1/2} \qquad (2.5)$$

or

$$D_e = \left[\frac{4 \times 10^6 Q}{\pi \eta_v V_e} + D_H^2\right]^{1/2} \qquad (2.5A)$$

where Q is the flow measured in gallons/minute (m^3/sec), V_e is the eye velocity in ft/sec (m/sec), D_e is the impeller eye diameter in inches (mm), D_H is the hub diameter in inches (mm) and η_v is the volumetric efficiency which is defined as:

$$\eta_v = \frac{Q}{Q + Q_L} \qquad (2.6)$$

where Q_L is the leakage flow measured in gallons/min (m^3/sec). The eye velocity v_e is usually chosen in the range of 5 to 20 ft/sec (1.5 to 6.0 metres/sec) [6]. To calculate the leakage flow Q_L, the details of the individual pump design must be known. For an approximate prediction of η_v at the design point, Figure 2.5 which shows the volumetric efficiency as a function of specific speed and flow for standard pumps may be used.

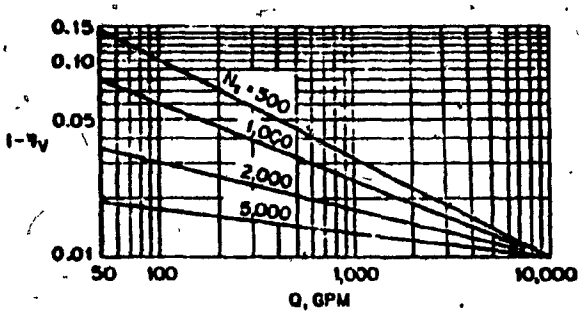

Figure 2.5 - Volumetric Efficiency as a Function of Specific Speed and Capacity.[7]

The inlet angle is defined as the ratio of meridional velocity c_{m_1} to the peripheral velocity u_1 shown in Figure 2.1(B). Therefore,

$$\text{Tan } \beta_1 = \frac{c_{m_1}}{u_1} \tag{2.7}$$

where β_1 is the vane inlet angle, c_{m_1} is the meridional velocity at the inlet in ft/sec (metre/sec) and u_1 is the peripheral velocity in ft/sec (metre/sec). Also:

$$u_1 = \frac{\pi D_e N}{720} \tag{2.8}$$

or

$$u_1 = \frac{\pi D_e N}{6 \times 10^4} \tag{2.8A}$$

The inlet vane angle affects the suction performance of the pump. Lower values are selected when low net positive suction head is required as in the case of boiler feed and condensate pumps. Net positive suction head is defined as the pressure available at the impeller eye above vapor pressure at the specified temperature. The vane angle is generally selected between 10°to 25°, independent of specific speed. A compromise between efficiency and cavitation results in a vane angle of 17° [8].

Measurements have shown that the discharge Q_n at the best efficiency point is not achieved due to the prerotation effects occuring prior to entering the blades [9]. In order to achieve the required discharge, it is found necessary to increase the blade angle β_1. The increase in angle β_1 can be calculated from the following equation [10]:

$$\text{Tan } \beta_1'(r) = \frac{\text{Tan } \beta_1}{\left[1 - \frac{Zt}{2\pi r \text{Sin}\beta_1'(r)}\right]} \qquad (2.9)$$

where β_1 is the vane angle in degrees, β_1' is the modified vane angle in degrees, Z is the number of vanes, t is the thickness of the vane in inches (mm) and r is the radius in inches (mm).

Some iterations are required to find a solution to the above equation. The number of vanes in the initial stages of the design can be assumed. There should be enough vanes to assure proper guidance of the liquid. Too many vanes will result in excessive frictional losses. The number of vanes generally used is between 5 and 12 [11].

The inlet width can be calculated from the following equation [12]:

$$b_1 = \frac{0.321Q}{\eta_v D_e c_{m_1} \varepsilon_1 \pi} \qquad (2.10)$$

or

$$b_1 = \frac{10^6 Q}{\eta_v D_e c_{m_1} \varepsilon_1 \pi} \qquad (2.10A)$$

where ε_1 is the contraction factor. The value of ε_1 is generally chosen between 0.8 and 0.9 [12] in the preliminary calculation of the impeller inlet width. After the number of vanes and their inlet thicknesses have finally been determined, the exact value of ε_1 may be found from [13]:

$$\varepsilon_1 = \frac{Zt}{\pi D_e \text{Sin}\beta_1'} \qquad (2.11)$$

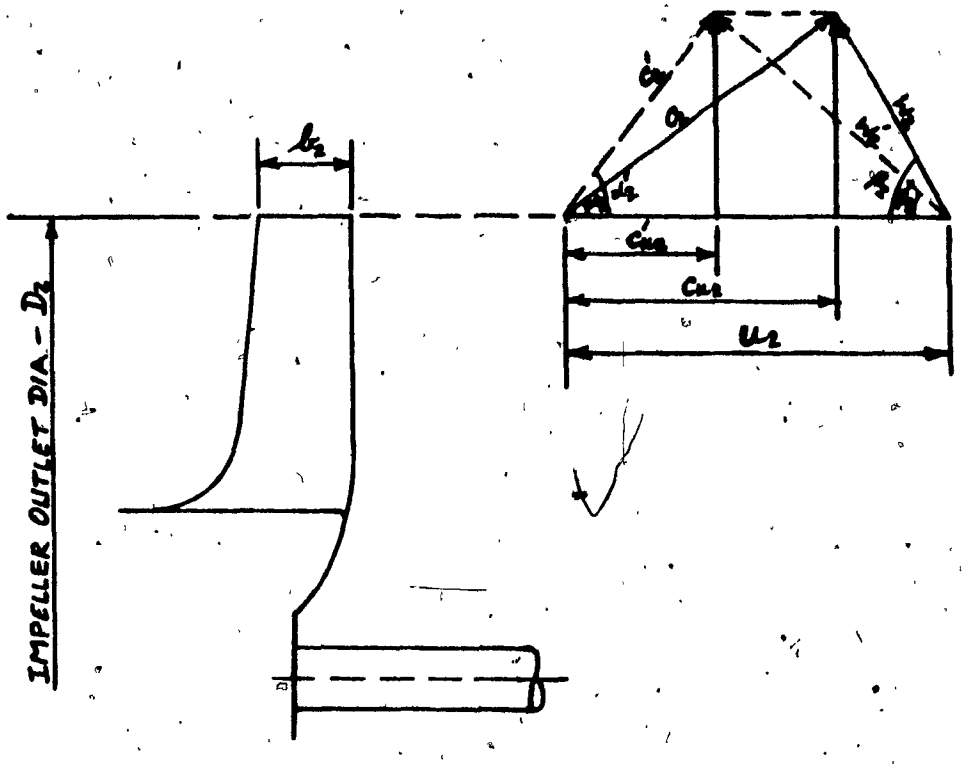

Figure 2.6 - Typical Outlet Section With Corresponding Outlet Velocity Triangle.

This completes the design of the inlet section. It should be pointed out that the number of vanes may be altered at the latter stages of the design and this will necessitate reconsideration of the parameters affected by this change.

2.2.2 Outlet Section

The outlet section is characterised by the impeller outlet diameter D_2 and the outlet width b_2. Figure 2.6 illsutrates a typical outlet section.

In order to arrive at the impeller outlet diameter D_2, the value of the peripheral velocity u_2 has to be calculated. The equation for calculating u_2 can be developed from the outlet velocity triangle (Fig. 2.3) as follows:

$$c_{u_2} = u_2 - c_{m_2} \text{Cot } \beta_2 \qquad (2.12)$$

where c_{u_2} is the theoretical component of the peripheral velocity in ft/sec (m/sec), u_2 is the peripheral velocity in ft/sec (m/sec), c_{m_2} is the outlet meridional velocity in ft/sec (m/sec) and β_2 is the outlet vane angle.

From equation (2.1)

$$c'_{u_2} = \mu c_{u_2} \qquad (2.13)$$

and substituting Equations (2.12) and (2.13) into Euler's equation yields

$$H = \mu \eta_H \frac{u_2^2}{g} \left(1 - \frac{c_{m_2}}{u_2} \text{Cot } \beta_2\right) \qquad (2.14)$$

The pump head H, as defined by Equation 2.14, can be made dimensionless by dividing with $\frac{u_2^2}{2g}$ resulting in the head coefficient [14]:

$$\psi = \frac{2gH}{u_2^2} = 2\mu\eta_H \left[1 - \frac{c_{m_2}}{u_2} \cot\beta_2\right] \tag{2.15}$$

The terms on the right-hand side of Equation 2.15 are either known or obtainable. Values of the ratio $\frac{c_{m_2}}{u_2}$ can be read from Figure 2.7 for different values of specific speed. Also, angle β_2 can be chosen from Figure 2.8 as a function of specific speed. The hydraulic efficiency η_H can be calculated from the following equation [15]:

$$\eta_H = 1 - \frac{0.8}{Q^{1/4}} \tag{2.16}$$

Numerous formulas have been proposed to compute the slip factor μ. Often, empirical coefficients are employed to bring the results into agreement with the available test data, as for example [17]:

$$\mu = 1 - \frac{\pi \sin\beta_2}{Z} \tag{2.17}$$

Equation 2.17 was proposed by Stodola for the case of zero flow, and it is frequently used in American pump design practice. Another formulation has been proposed by Pfleiderer [18]:

$$\mu = \frac{1}{1 + \frac{a}{Z}\left[1 + \frac{\beta_2}{60}\right] \frac{2}{1-(R_1/R_2)^2}} \tag{2.18}$$

where a is a coefficient, R_1 is the inlet radius in inches (mm) and R_2 is the outlet radius in inches (mm).

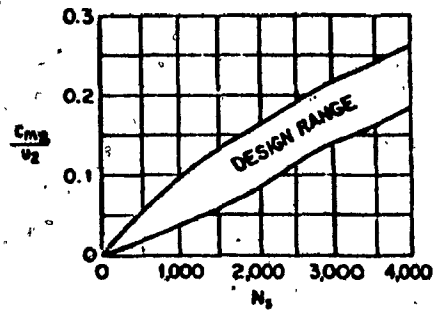

Figure 2.7 - $\frac{c_{m_2}}{u_2}$ Versus Specific Speed [16]

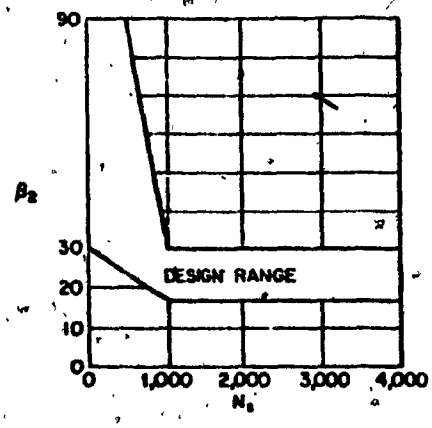

Figure 2.8 - Impeller Discharge Angle Versus Specific Speed [16].

The slip factor is affected not only by the impeller configuration, but also by the interaction of the diffusing system with the impeller. Pfleiderier, on the basis of a series of tests, defines the coefficient a in Equation 2.18 in terms of the casing design. For volutes, a = .65 to .85. Corresponding values of the slip factor vary between 0.65 and 0.75 for radial type of impellers [19].

The outlet diameter of impeller can be calculated from:

$$D_2 = \frac{720u_2}{\pi N} \tag{2.19}$$

or

$$D_2 = \frac{6 \times 10^4 u_2}{\pi N} \tag{2.19A}$$

The outlet width b_2 is calculated in a way similar to the inlet width. The value of b_2 can be calculated from the following equation [20]:

$$b_2 = \frac{0.321Q}{\pi \eta_v D_2 c_{m_2} \epsilon_2} \tag{2.20}$$

or

$$b_2 = \frac{10^6 Q}{\pi \eta_v D_2 c_{m_2} \epsilon_2} \tag{2.20A}$$

where ϵ_2 is the outlet contraction factor. The outlet contraction factor is assumed in the preliminary calculation subject to a correction after the actual thickness and the number of vanes have been determined.

The factor ϵ_2 is usually between 0.90 to 0.95 [20]. The exact value of ϵ_2 may be found from the equation [21]

$$\epsilon_2 = 1 - \frac{Zt}{\pi D_2 \sin \beta_2} \tag{2.21}$$

2.2.3 Vanes

The number of vanes can be verified with the following equation

$$Z = 6.5 \frac{D_2 + D_e}{D_2 - D_e} \sin \frac{\beta_1 + \beta_2}{2} \tag{2.22}$$

The number of vanes generally used is between 5 and 12 [22]. A smaller number of vanes is employed to give a steeper falling curve or a smaller output from the same casing [23].

The vane angles and diameters having been established, the next step is to construct the vane shape. There are three principal methods for determining the vane shape. Circular arc, point-by-point and conformal representation. The details of the point-by-point method and the conformal representation method are detailed in [24]. Circular arc method [25] will be outlined here in order to provide a brief outline of the steps involved.

In this method, the impeller is divided into a number of assumed concentric rings not necessarily equally spaced between R_e and R_2. The radius ℓ of the circular arc obtained in any ring is

$$\ell = \frac{R_b^2 - R_a^2}{2(R_b \cos \beta_b - R_a \cos \beta_a)} \tag{2.23}$$

where R_a is the radius of the inner ring, R_b is the radius of the

outer ring, β_b is the angle at radius R_b and β_a is the angle at radius R_a. Inlet and outlet angle β is known and a curve is drawn between angle β and the radii. The vane angles at R_a and R_b are taken from the curve. Since adjacent arcs are tangent to each other, both their centres will be on the same line through the point of tangency.

CHAPTER 3

CASING DESIGN

CHAPTER 3

CASING DESIGN

3.1 Casing-Volute Type

The purpose of the volute is to convert the kinetic energy of the water leaving the impeller into the corresponding pressure head. There are several design elements of the volute casing which determine its hydraulic characteristics namely, volute area, volute width, tongue angle and base circle. The base circle is the circle described by the impeller outlet radius R_2 and is the reference circle from which volute areas are measured.

The first step in the design of the volute involves the determination of the throat area. This is calculated from the continuity equation as

$$A_{th} = \frac{0.321Q}{C_{th}} \qquad (3.1)$$

or

$$A_{th} = \frac{10^6\, Q}{C_{th}} \qquad (3.1A)$$

where A_{th} is the throat area in square inches (mm^2), Q is the flow in gallons per minute ($metre^3/sec$) and C_{th} is the throat velocity in ft/sec (metre/sec). The throat velocity C_{th} is selected from Figure 3.1 which is a plot of empirical findings versus specific speed.

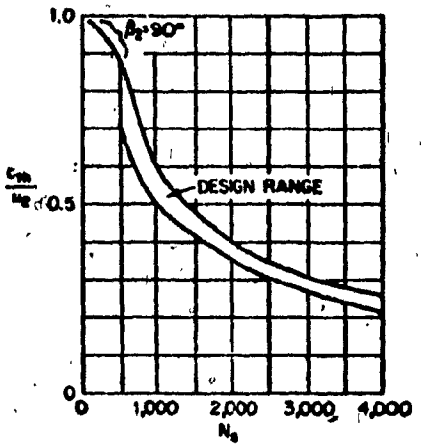

Figure 3.1 - C_{th}/u_2 Versus Specific Speed [27].

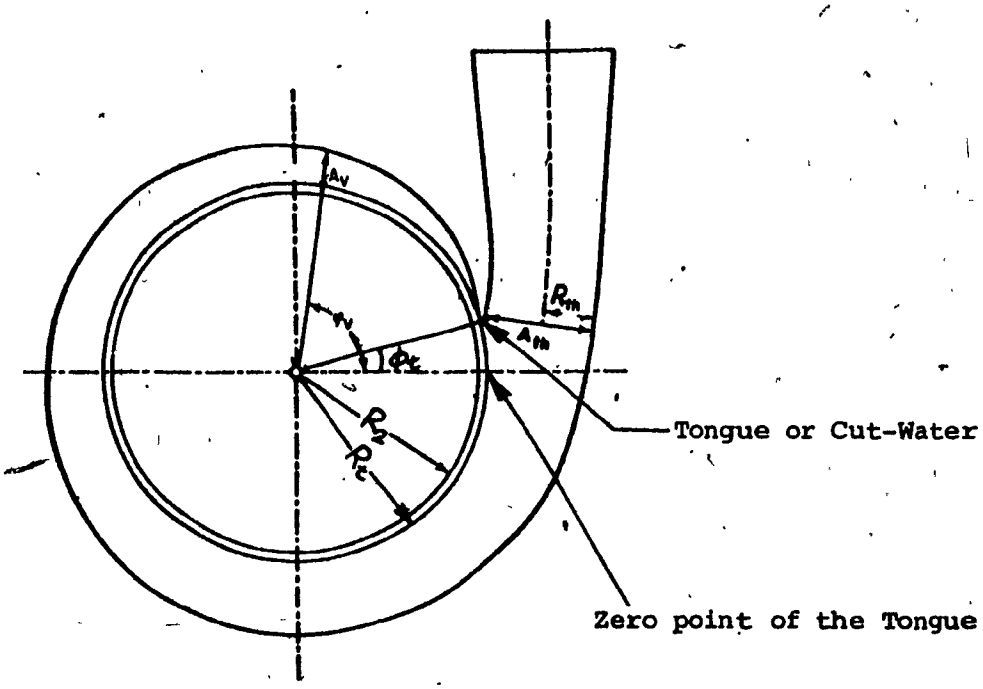

Figure 3.2 - Volute Casing

Referring to Figure 3.2, it is apparent that the total pump capacity Q must be accomodated through the volute throat. The flow Q_v past any section of the volute is

$$Q_v = \frac{\phi_v}{360} \times Q$$

where ϕ_v is the angle in degrees measured from the zero point of the volute. Assuming constant mean velocity of flow for all volute sections, the volute areas are proportional to the central angle ϕ_v [26]. Therefore

$$A_v = \frac{\phi_v}{360} \times A_{th} \qquad (3.2)$$

where A_v is the volute area in square inches (mm^2). After establishing the volute area A_v, the dimensions of the volute section can be determined once the shape of the volute section has been selected. The volute section shape can be circular, rectangular or trapezoidal. The choice of shape does not greatly influence the pump performance [28]. The most commonly used shape is a trapezoidal one, since it is claimed to be slightly more efficient than the other two shapes. The rectangular shape is employed in cases where the flexibility of using the same casing with different impellers having different outlet widths is a prerequisite. For illustrative purposes, the procedure of establishing the volute section dimensions for a rectangular shape is as follows:

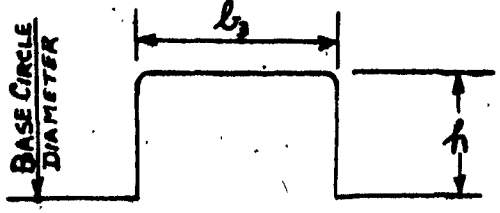

Figure 3.3 - Volute Shape Section

Referring to Figure 3.3, the volute width b_3 is two to three times the impeller discharge width [29]. After choosing the volute width b_3, the volute height h is found from

$$h = \frac{A_v}{b_3} \tag{3.3}$$

The tongue angle ϕ_t (Figure 3.2) may be found by assuming that the flow follows a logarithmic spiral the contour of which is defined by [30]

$$R = R_2 e^{\tan \alpha_2' \bar{\phi}} \tag{3.4}$$

where $\bar{\phi}$ is the angle measured in radians and e is the base of natural logarithms. Taking log of both sides of the above equation and for the tongue radius R_t,

$$\phi_t^\circ = \frac{132 \ \mathrm{Log}_{10} R_t/R_2}{\mathrm{Tan}\alpha_2'} \tag{3.5}$$

To avoid turbulence, excessive noise and to allow the velocities of the water leaving the impeller to stabilize before coming into contact with the tongue, the radius R_t is 5 to 10% greater than the impeller outside radius R_2 [30].

Finally, the volute terminates in a divergent diffuser shown schematically in Figure 3.4, with a taper angle α_3 in the 6° to 10° range.

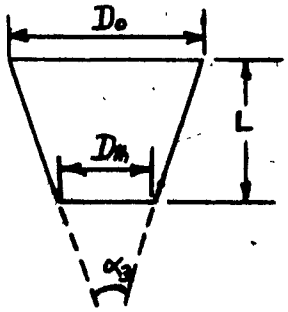

Figure 3.4 - Volute Diffuser

The taper angle α_3 is defined by

$$\text{Tan } \frac{\alpha_3}{2} = \frac{D_o - D_{th}}{2L} \qquad (3.6)$$

where D_o is the outlet diameter of the diffuser, D_{th} is the throat diameter and L is the length of the diffuser. Typical values of α_3 as a function of the throat velocity are given in Figure 3.5.

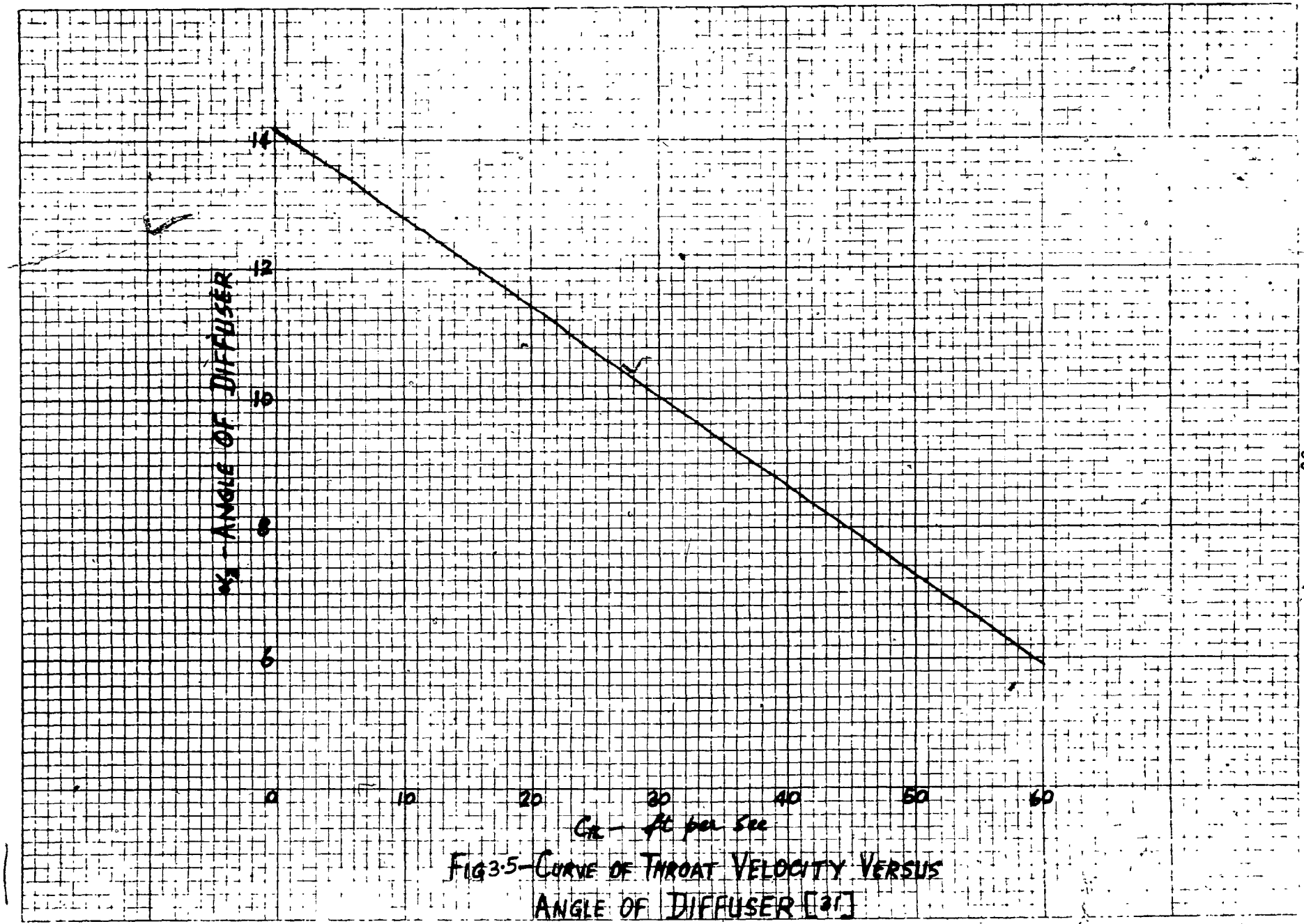

FIG 3.5 - CURVE OF THROAT VELOCITY VERSUS ANGLE OF DIFFUSER [31]

CHAPTER 4

UNBALANCED FORCES

CHAPTER 4

UNBALANCED FORCES

4.1 Unbalanced Forces Developed in Pump Casing

Two types of forces develop around the impeller in a centrifugal pump casing. One force acts radially on the impeller periphery and causes the pump shaft to deflect. The other acts axially on the sides of the impeller and puts the pump shaft in compression or tension. The radial force arises from the unbalanced pressure distribution around the periphery of the impeller. The axial force is due to the difference between the force resultants acting on either side of the impeller. The direction of the net axial force depends on the design of the impeller and the pressure at the pump suction.

4.1.1 Radial Thrust

The pressure on the inlet circumference of the volute casing is not uniform everywhere, even at the normal discharge of the pump. This leads to an unbalanced radial force which acts on the pump shaft. This force is called the radial thrust and attains a minimum in the region of the normal operating point. It varies with the discharge ratio and attains a maximum value when the discharge Q is zero. Radial thrust causes additional deflection of the shaft in a horizontal pump in addition to that due to the dead weight of the elements mounted on it. The presence of radial thrust leads to rapid wear of bearings, leakage from the gland and eventual failure of the shaft due to fatigue. The

magnitude of radial thrust can be calculated from the following equation [32]:

$$F_r = K_r p D_2 B_2 \qquad (4.1)$$

where F_r is radial thrust in pounds (Newton), K_r is experimental coefficient, p is pressure generated by the pump in pounds per square inch (N/mm^2) and B_2 is outlet breadth of impeller including shrouds in inches (mm). The value of K_r can be read from Figure 4.1.

4.1.2 Axial Thrust

Axial loads are developed as a result of the pressure variations existing in the pump casing and its effect on the exposed areas of the impeller and shaft. Axial thrust is the summation of unbalanced forces on an impeller acting in the axial direction. Figure 4.2 illustrates the axial thrust qualitatively.

The axial forces acting on a double suction impeller are balanced due to the symmetrical construction. Theoretically, a double suction impeller is in hydraulic balance (Figure 4.2). In a single-suction impeller with the shaft passing through the impeller eye (Figure 4.3), the axial thrust develops as a result of the pressure acting on the back shroud being higher than the pressure on the other side. The axial force acts towards the suction and is equal to the product of the net pressure generated by the impeller and the unbalanced annular area (Figure 4.3). The magnitude of the suction pressure in these pumps does not affect the resulting axial thrust. But in an overhung, single suction impeller (Figure 4.4), the axial forces are definitely affected by the

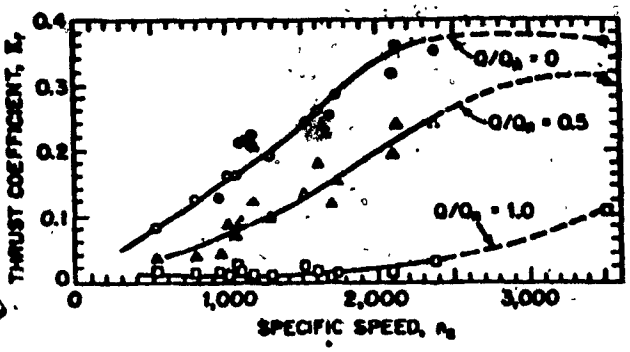

Figure 4.1 - K_r as a Function of Specific Speed and Capacity for Single Volute Pump [33].

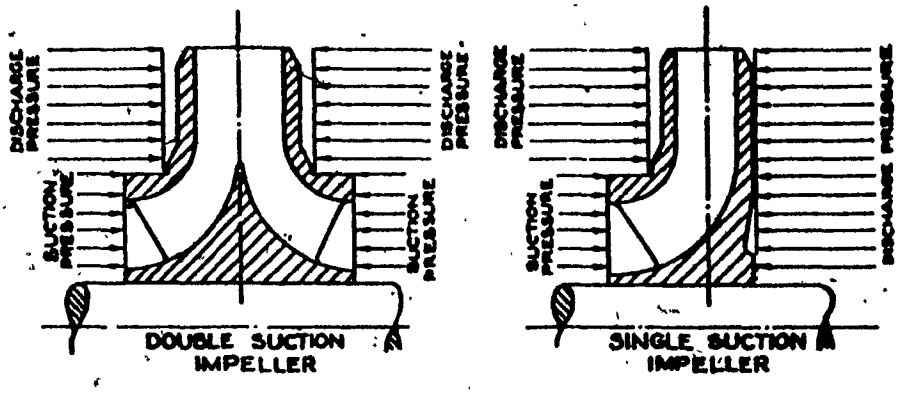

Figure 4.2 - Origin of Pressure Acting on Impeller Shrouds to Produce Axial Thrust [34].

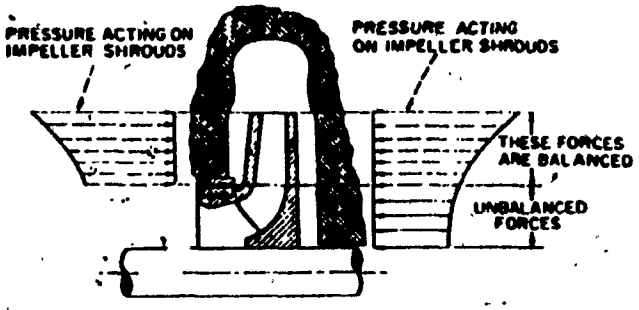

Figure 4.3 - Actual Pressure Distribution on Front and Back Shrouds of Single Suction Impeller With Shaft Through Impeller Eye [35].

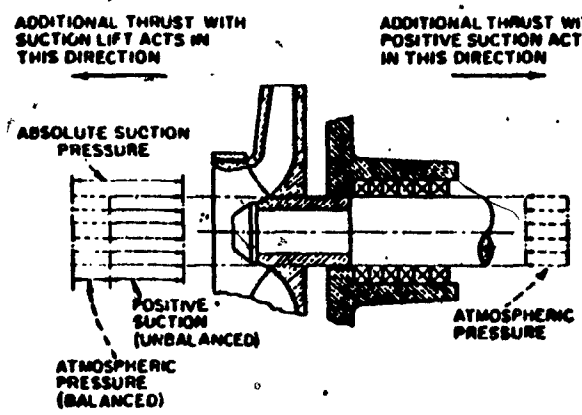

Figure 4.4 - Axial Thrust in Single-Suction Overhung Impeller [36].

suction pressure. In addition to the unbalanced force found in a single suction impeller with the shaft through the impeller eye (Figure 4.3), there is an axial force equivalent to the product of the shaft area through the stuffing box and the difference between suction and atmospheric pressure. This force acts towards the impeller suction when the suction pressure is less than atmospheric or in the opposite direction when it is higher than atmospheric.

The axial thrust in a single suction impeller is balanced by providing front and back wearing rings of equal diameters and drilling balancing holes in the impeller shroud (Figure 4.5). These holes offset the pressure in spaces 1 and 2. The other alternative is to connect space 2 with space 1 by means of an external pipe. This is sometimes used in large pumps in order to avoid local leakage flow which opposes the main flow in impeller suction. In pumps handling gritty liquids, the pump out vanes or radial ribs fitting closely to the casing (Figure 4.6) , are cast on to the back shroud. The effect of these vanes is to reduce the pressure acting on the back shroud of the impeller.

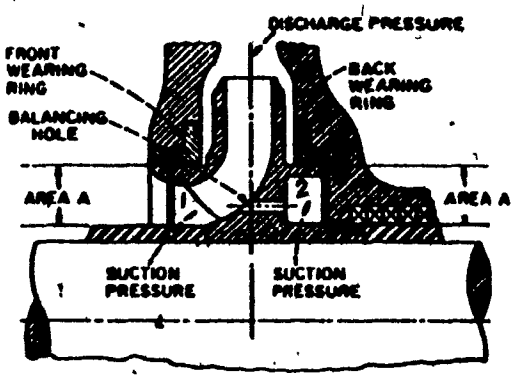

Figure 4.5 - Balancing Axial Thrust of Single-Suction Impeller by Means of Wearing Ring on Back Side and Balancing Holes [37].

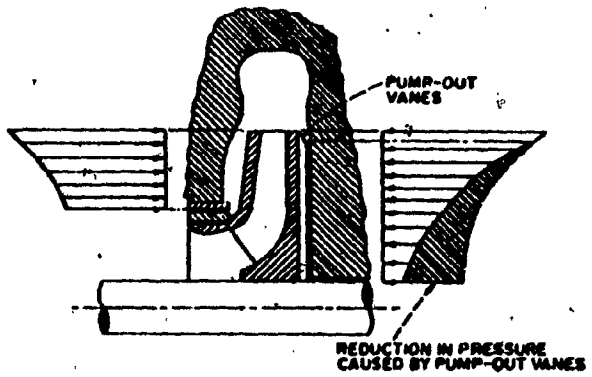

Figure 4.6 - Effect of Pump-Out Vanes in a Single-Suction Impeller to Reduce Axial Thrust [37].

CHAPTER 5

MECHANICAL DETAILS

CHAPTER 5

MECHANICAL DETAILS

5.1 Casing

In small pumps, the casing thickness is dictated by the limitations of the metal casting process and not by strength consideration. The situation is completely different, however, for large pumps. In this case the calculations are quite cumbersome in view of the complicated shapes of the various elements.

Excessive wall thickness unnecessarily increases the weight and cost. Apart from this, it may lead to fabrication problems. The ideal design is one in which the material is uniformly ditributed which implies a very small fluctuation in operating stresses.

The stress distribution in the walls of pump elements under pressure is determined by various methods based on the measurement of local strain. These experimental values are used to equalize the stress distribution in subsequent elements by reducing the thickness in some places and increasing it in others. Sometimes, stiffening ribs are added to increase the strength of the casting in order to keep the thickness to a minimum value.

5.2 Impeller

Impellers are usually cast iron, although material selection depends on applications. The shroud of pump impellers of average peripheral

speeds ($u_2 \leq 100$ ft/sec) do not require any special calculations since the working stresses do not exceed those which are permissible for casting thickness. For higher peripheral speeds, it is essential to calculate accurately the dynamic stresses [38].

All centrifugal pump impellers should be balanced statically to keep eccentricity in the impeller to a minimum and to prevent shaft whip. Static balancing alone removes unbalanced static moments but does not remove unbalanced dynamic moments. The latter can be detected only through the use of a dynamic balancing machine. As a rule, large size impellers, especially when operated at higher speeds are balanced dynamically.

5.3 Shaft

The shaft is subjected to torsional forces due to the transmitted torque, bending moments due to dead loads, radial thrust, forces due to imperfect balancing of the rotating masses and lastly, axial thrust.

The deflection of the shaft should be kept as small as practical and it should in fact be less than the clearances allowed between the stationary and the rotating parts. The shaft must be checked to assure that no resonances occur under normal operating speeds. The rotational speeds at which resonances occur are designated as critical speeds.

5.4 Critical Speed

The critical speed for an impeller-shaft assembly is of interest when it is in the range of the operating speed of the pump. In pump construction, only the first critical speed is of importance and

critical speeds of higher orders are not taken into account. The shaft-impeller should be so designed that the operating speed is not an even fraction or multiple of the pump's first critical speed. Neglecting gyroscopic effects, bearing elasticity and stiffening due to impeller hub and shaft sleeves, the first critical speed can be calculated from [39]:

$$N_c = 187.5 \left[\frac{\Sigma Wy}{\Sigma Wy^2} \right]^{1/2} \qquad (5.1)$$

where N_c is the first critical speed in rpm, W is load in pounds (Kg) and y is the deflection in inches (mm). For the most part, pump shafts are stepped having variable cross-sections. Graphical methods of finding the deflections in stepped shafts are probably the most widely used. A numerical method of carrying out the same steps as in the graphical method has been proposed by Hopkins [40]. The deflection y appearing in Equation 5.1 can be found by modelling the shaft as a straight beam from:

$$\frac{d^2y}{dx^2} = \frac{M}{EI} \qquad (5.2)$$

where M is the bending moment in pound-inches (Kg-mm), E is the modulus of elasticity in pounds per square inch (N/mm^2) and I is the moment of inertia in inches^4 (mm^4). In applying Equation 5.2, the integration constants are determined by the type of boundary conditions which apply to the configuration considered.

5.5 Bearings

In order to select the appropriate bearings, the load to be carried by each bearing must be known. This involves a static analysis of the shaft assembly. There are two standard arrangements for supporting pump rotors: Impeller overhung on two bearings and impeller between two bearings. For the overhung case, shown in Figure 5.1, the static analysis yields:

$$F_1 = \frac{W \times (l_1 + l_2)}{l_2} \qquad (5.3)$$

$$F_2 = \frac{W \times l_1}{l_2} \qquad (5.4)$$

where F_1 is the reaction on the inboard bearing in pounds (Kg), F_2 is the reaction on the outboard bearing in pounds (Kg), l_1 is the overhung length in inches (mm) and l_2 is the distance between two bearings in inches (mm).

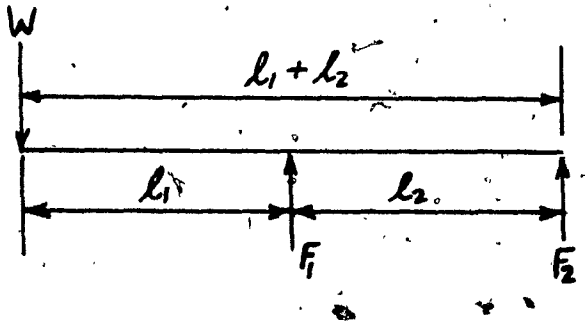

Figure 5.1 - Impeller Overhung on Two Bearings.

For the impeller between two bearings, as shown in Figure 5.2, we have:

$$F_1 = \frac{W \times l_2}{l_1 + l_2} \qquad (5.5)$$

$$F_2 = \frac{W \times l_1}{l_1 + l_2} \qquad (5.6)$$

If $l_1 = l_2$, then $F_1 = F_2 = \frac{W}{2}$.

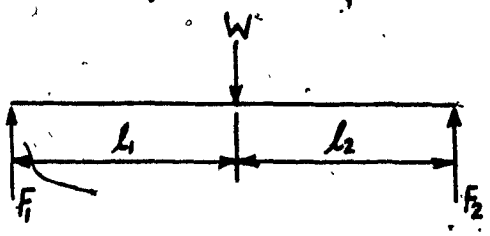

Figure 5.2 - Impeller Between Two Bearings.

Since the radial thrust does not act vertically, W is taken as the vector sum of impeller weight and radial thrust. Axial loads are also taken into account when selecting bearings. Once the equivalent loads have been established, bearings can be selected for any number of operating hours.

CHAPTER 6

CONCLUSION

CHAPTER 6

CONCLUSION

Conclusion

The practical approach to the design of centrifugal pumps presented is based on one dimensional analysis. Refinements to this approach can be made to improve the design. The same problem can be attacked in a number of ways. Each way gives a slightly different solution. All of these solutions may not be of equal merit when considered from the point of view of efficiency and production costs.

One will notice the large number of variables involved. It is necessary to assume some of the values of these variables. Optimum results are most likely to be obtained for given operating conditions when the variables are chosen on the basis of experimental tests on existing pumps which have given high efficiencies. Calculations of the dimensions of the pump may also be based on the results of tests on model pumps. Consequently, the skill and experience of the designer will provide the optimum design as a compromise between high efficiency with low running power cost and low production costs to secure a job against severe competition.

REFERENCES

REFERENCES

1. Karasik, I.J., Pump Handbook, McGraw Hill Book Company, 1976; pp. 2-26.
2. Church, A.H., Centrifugal Pumps and Blowers, John Wiley and Sons Inc., New York, 1944; p. 49.
3. Ibid: Number 1, pp. 2-10.
4. Ibid: Number 2, p. 93.
5. Ibid: Number 2, p. 94.
6. Lazarkiewicz, S. and Troskolanski, A.T., Impeller Pumps, Parmagon Press, Oxford, London, 1962; p. 133.
7. Ibid: Number 1, pp. 2-18.
8. Ibid: Number 1, pp. 2-12.
9. Ibid: Number 6, p. 134.
10. Ibid: Number 1, pp. 2-13.
11. Anderson, H.H., Centrifugal Pumps, Trade and Technical Press Limited, 1962; p. 436.
12. Ibid: Number 2, p. 95.
13. Ibid: Number 2, p. 106.
14. Ibid; Number 1, pp. 2-9.
15. Ibid: Number 1, pp. 2-19.
16. Ibid: Number 1, pp. 2-12.
17. Ibid: Number 1, pp. 2-7.
18. Ibid: Number 1, pp. 2-8.
19. Ibid: Number 2, p. 98.
20. Ibid: Number 2, p. 99.
21. Ibid: Number 2, p. 106.

22. Ibid: Number 6, p. 127.

23. Ibid: Number 11, p. 436.

24. Ibid: Number 2, p. 99.

25. Ibid: Number 6, p. 166.

26. Stepanoff, A.J., Centrifugal and Axial Flow Pumps, John Wiley and Sons, Inc., 1964; p. 112.

27. Ibid: Number 1, pp. 2-15.

28. Worster, R.C., "The Flow in Volutes and Its Effect on Centrifugal Pump Performance", Proceedings of the Institute of Mechanical Engineers, Vol. 177, No. 31, 1963; p. 853.

29. Ibid: Number 1, pp. 2-16.

30. Ibid: Number 2, p. 120.

31. Ibid: Number 8, p. 282.

32. Ibid: Number 6, p. 359.

33. Ibid: Number 1, pp. 2-175.

34. Ibid: Number 1, pp. 2-59.

35. Ibid: Number 1, pp. 2-60.

36. Ibid: Number 1, pp. 2-62.

37. Ibid: Number 1, pp. 2-61.

38. Kovats, A., Design and Performance of Centrifugal and Axial Flow Pumps and Compressors, The Macmillan Company of New York, New York, 1964; p. 432.

39. Ibid: Number 26, p. 347.

40. Hopkins, R.B., "Stepped Shaft and Non-Uniform Beams", Machine Design, July 6, 1961; p. 159.

41. Oberg & Jones, Machinery Handbook, Industrial Press Inc., New York, 1968; p. 460.

42. SKF Catalogue, Published by Canadian SKF Company Ltd.; 1961; p. 17.

43. Ibid: Number 42, p. 11.

44. Ibid: Number 42, p. 13.

45. Ibid: Number 42, p. 18.

46. Ibid: Number 42, p. 84.

47. Ibid: Number 40, p. 164.

APPENDIX

DESIGN EXAMPLE

APPENDIX

DESIGN EXAMPLE

Data

The pump will be designed to develop a head of 130 feet and deliver 500 gallons per minute of water at 68°F. It is to be directly connected to a motor operating at 1750 rpm.

Specific Speed

$$N_s = \frac{N\sqrt{Q}}{H^{3/4}}$$

$$= \frac{1750\sqrt{500}}{130^{3/4}}$$

$$= 1016$$

Inlet Dimensions

The brake horsepower is (Equation 2.3)

$$BHP = \frac{Q \times H \times SG}{3960 \times \eta}$$

Value of η is read from Figure 1.5 and is equal to 75%. Therefore,

$$BHP = \frac{500 \times 130 \times 1}{3960 \times 0.75}$$

$$= 21.9 \text{ hp}$$

A motor is available with 30 hp. So 30 hp will be the maximum horsepower used. The shaft torque is (Equation 2.2):

$$T = \frac{63000 \times BHP}{N}$$

$$= \frac{63000 \times 30}{1750}$$

$$= 1080$$

The shaft is made of commercial steel. The allowable shear stress S_s for commercial steel is 6000 psi [41]. The shaft diameter is (Eq. 2.4)

$$D_s = \left[\frac{5.1T}{S_s}\right]^{1/3}$$

$$= \frac{5.1 \times 1080}{6000}^{1/3}$$

$$= 0.972 \text{ inches, or } 1.0 \text{ inch.}$$

To take care of bending moments and to keep critical speed high, increase D_s to 1.25 inches. This diameter will be confirmed after the critical speed analysis.

The hub does not protrude into the eye, so the hub diemater D_H is zero. The eye diameter can be calculated from (Equation 2.5):

$$D_e = \left[\frac{1.280}{\pi \eta_v v_e} + D_H\right]^{1/2}$$

v_e is taken as 10 ft/sec. η_v is read from Figure 2.5 and is equal to 97%.

$$D_e = \left[\frac{1.28 \times 500}{\pi \times .97 \times 10} + 0\right]^{1/2}$$

$$= 4.597 \text{ inches, or } 4\frac{5}{8}".$$

The inlet angle β_1 is (Equation 2.7)

$$\tan \beta_1 = \frac{cm_1}{u_1}$$

cm_1 is equal to v_e. Therefore, cm_1 is 10 ft/sec and

$$u_1 = \frac{\bar{\Lambda} D_e N}{720}$$

$$= \frac{\bar{\Lambda} \times 4.625 \times 1750}{720}$$

$$= 35.32 \text{ ft/sec}$$

Therefore, $$\tan \beta_1 = \frac{10}{35.32}$$

$$\beta_1 = 15.8°$$

The angle β_1 is increased somewhat to account for prerotation. This increase can be estimated from (Eq. 2.9)

$$\tan \beta_1'(r) = \frac{\tan \beta_1}{\left[1 - \frac{Zt}{Z\bar{\Lambda} r \sin \beta_1'(r)}\right]}$$

Taking vane thickness t to be constant and equal to 3/16", assume number of vanes Z as 5. The number of vanes will be verified later on.

$$\tan \beta_1' = \frac{\tan 15.8}{\left[1 - \frac{5 \times .1875}{\bar{\Lambda} \times 4.625 \sin \beta_1'}\right]}$$

After some iterations $\beta_1' = 19.4°$

The inlet width is (Equation 2.10):

$$b_1 = \frac{.321\ Q}{\bar{\Lambda}\ De\ cm_1\ \eta_v\ \varepsilon_1}$$

Inlet contraction factor ε_1 is assumed initially. The exact value of ε_1 is found later on, after the number of vanes have been verified. Assume ε_1 as 0.8. Therefore,

$$b_1 = \frac{.321 \times 500}{\bar{\Lambda} \times 4.625 \times 10 \times .97 \times 0.8}$$

$$= 0.1423 \text{ inches, say } 1\tfrac{3}{8} \text{ inches.}$$

Outlet Dimensions

The slip factor is (Equation 2.17)

$$\mu = 1 - \frac{\bar{\Lambda} \sin \beta_2}{Z}$$

$$\beta_2 = 24° \text{ (from Figure 2.8)}$$

$$\mu = 1 - \frac{\sin 24}{5}$$

$$= 0.744$$

The value of μ lies within 0.65 to 0.75 and is accepted. The head coefficient ψ is (Equation 2.15):

$$\psi = 2 \mu \eta_H (1 - \frac{cm_2}{u_2} \cot \beta_2)$$

Where,

$$\eta_H = 1 - \frac{0.8}{Q^{1/4}}$$

$$= 1 - \frac{0.8}{500^{1/4}}$$

$$= 0.83$$

and

$$\frac{cm_2}{u_2} = 0.07 \text{ (value read from Figure 2.7)}$$

$$\psi = 2 \times 0.744 \times .83 (1 - 0.07 \cot 24)$$

$$\psi = 1.04$$

The peripheral velocity u_2 is (Equation 2.15)

$$u_2 = \left[\frac{2gH}{\psi}\right]^{1/2}$$

$$= \left[\frac{2 \times 32.2 \times 130}{1.04}\right]^{1/2}$$

$$= 89.7 \text{ ft/sec}$$

Thus, impeller outlet diameter

$$D_2 = \frac{720 \times u_2}{\overline{\Lambda} \times N}$$

$$= \frac{720 \times 89.7}{\overline{\Lambda} \times 1750}$$

$$= 11.747\text{" say } 11\ 3/4 \text{ inches.}$$

The outlet width is (Equation 2.20):

$$b_2 = \frac{.321\ Q}{\overline{\Lambda}\ \eta_v\ cm_2\ D_2\ \varepsilon_2}$$

Now, $$\frac{cm_2}{u_2} = 0.07$$

Therefore, $$cm_2 = .07 \times 89.7$$

$$= 6.279 \text{ ft/sec}$$

Outlet contraction factor ε_2 can be estimated from (Equation 2.21):

$$\varepsilon_2 = 1 - \frac{Zt}{\overline{\Lambda}\ D_2 \sin \beta_2}$$

$$= 1 - \frac{5 \times .1875}{\overline{\Lambda} \times 11.75 \times \sin 24}$$

$$= .938 \text{ say } 0.94$$

Value of ϵ_2 lies between 0.9 and 0.95 and so, above value of ϵ_2 can be used. It must be reminded that this value will be confirmed after the number of vanes are verified. Therefore,

$$b_2 = \frac{.321 \times 500}{\Lambda \times .97 \times 6.3 \times 11.75 \times .94}$$

$$= 0.757 \text{ inches say } 3/4 \text{ inches}$$

Finally, the number of vanes can be verified so that the assumed values of inlet and outlet contraction factor can be confirmed. The equation is (Equation 2.22):

$$Z = 6.5 \frac{D_2 + D_e}{D_2 - D_e} \sin \left(\frac{\beta_1^1 + \beta_2}{2}\right)$$

$$= 6.5 \frac{11.75 + 4.625}{11.75 - 4.625} \sin \left(\frac{19.4 + 24}{2}\right)$$

$$= 5.523$$

If number of vanes are taken as 6, then the value of ϵ_1 calculated by Equation (2.11) does not lie within 0.8 to 0.9. Therefore, the assumed number of vanes can be taken as correct.

Velocity Diagrams

All the ingredients for constructing the velocity diagrams are known. The inlet and the outlet velocity triangles can be drawn.

Inlet Triangle

$\beta_1 = 15.8°$, $\beta_1^1 = 19.4°$, $c_{m_1} = 10$ ft/sec, $u_1 = 35.35$ ft/sec and

cm_1^1 = 12.43 ft/sec. See Fig. A-1(A).

Outlet Triangle

$\beta_2 = 24°$, $cm_2 = 6.3$ ft/sec, $u_2 = 89.7$ ft/sec, $cu_2 = u_2 - cm_2 \cot \beta_2 =$ 75.5 ft/sec, $cu_2 = \mu \times cu_2 = 56.2$ ft/s and $\alpha_2' = \tan^{-1} \frac{cm_2}{cu_2} = \tan^{-1} \frac{6.3}{56.2} =$ 6.4°. See Figure A-1(B).

Design of Vanes

The radius of the circular arc is (Equation 2.23).

$$\ell = \frac{R_b^2 - R_a^2}{2(R_b \cos \beta_b - R_a \cos \beta_a)}$$

Values of R is selected between $R_e = 2.3125"$ and $R_2 = 5.875$ inches. β_1 and β_2 are known at R_e and R_2. A curve is drawn of β versus radius R and intermediate values of β are read from graph (Figure A-2).

R	R^2	β	cos β	R cos β	$R_b \cos \beta b - R_a \cos \beta a$	$R_b - R_a$	ℓ
2.3125	5.35	19.4	.943	2.181			
					1.146	7.34	3.20
3.5625	12.69	21	.934	3.327			
					2.043	21.83	5.34
5.875	34.52	24	.914	5.370			

Figure A-3 represents the impeller drawing.

SCALE: 1" = 20 ft/s

FIG A-1(A) INLET VELOCITY TRIANGLE

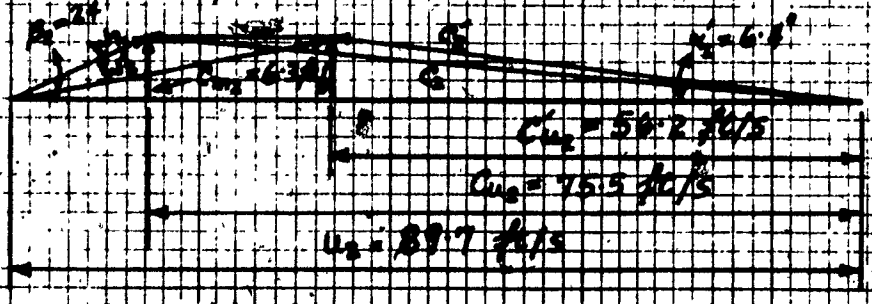

FIG A-1(B) - OUTLET VELOCITY TRIANGLE

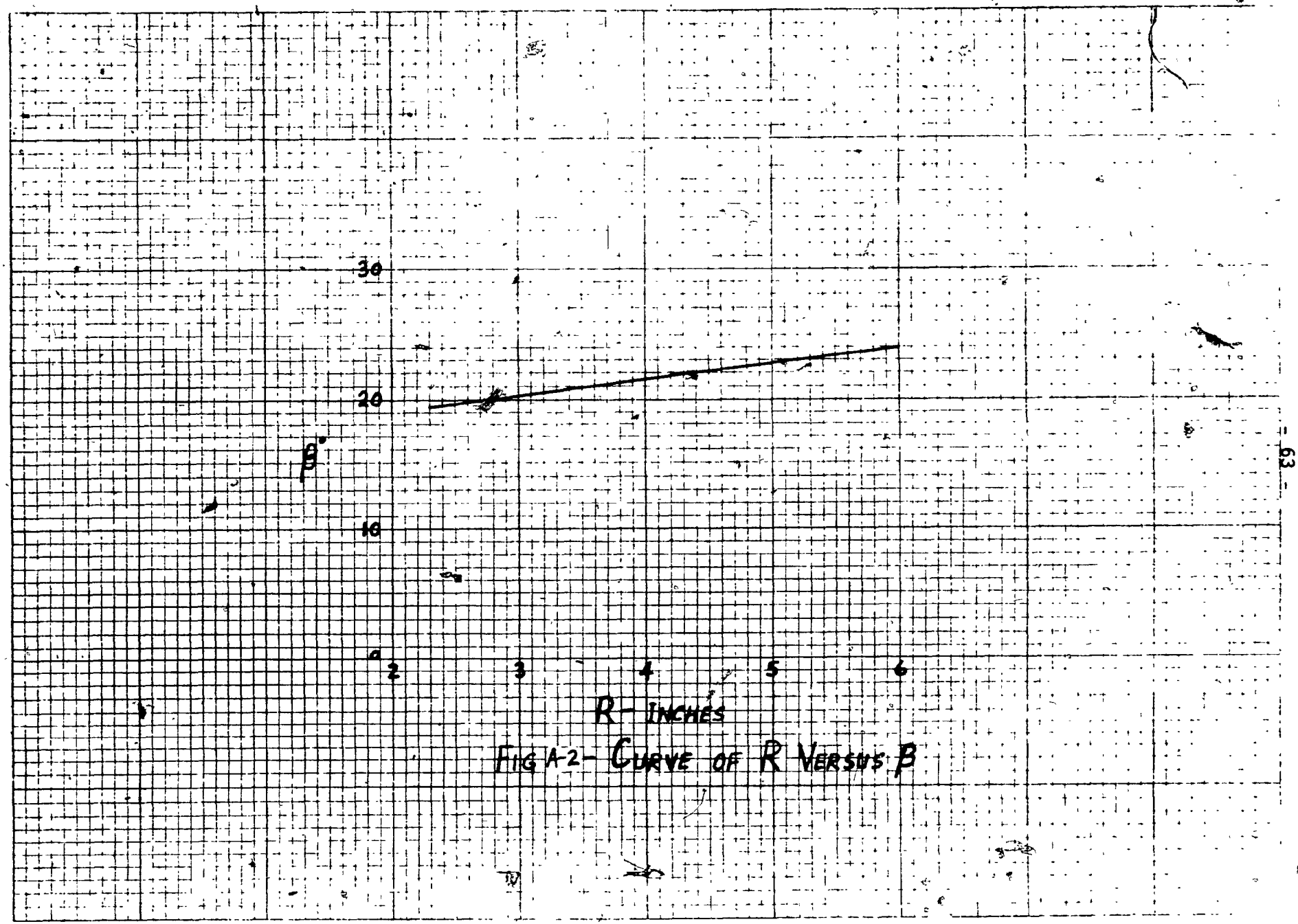

FIG A-2- CURVE OF R VERSUS β

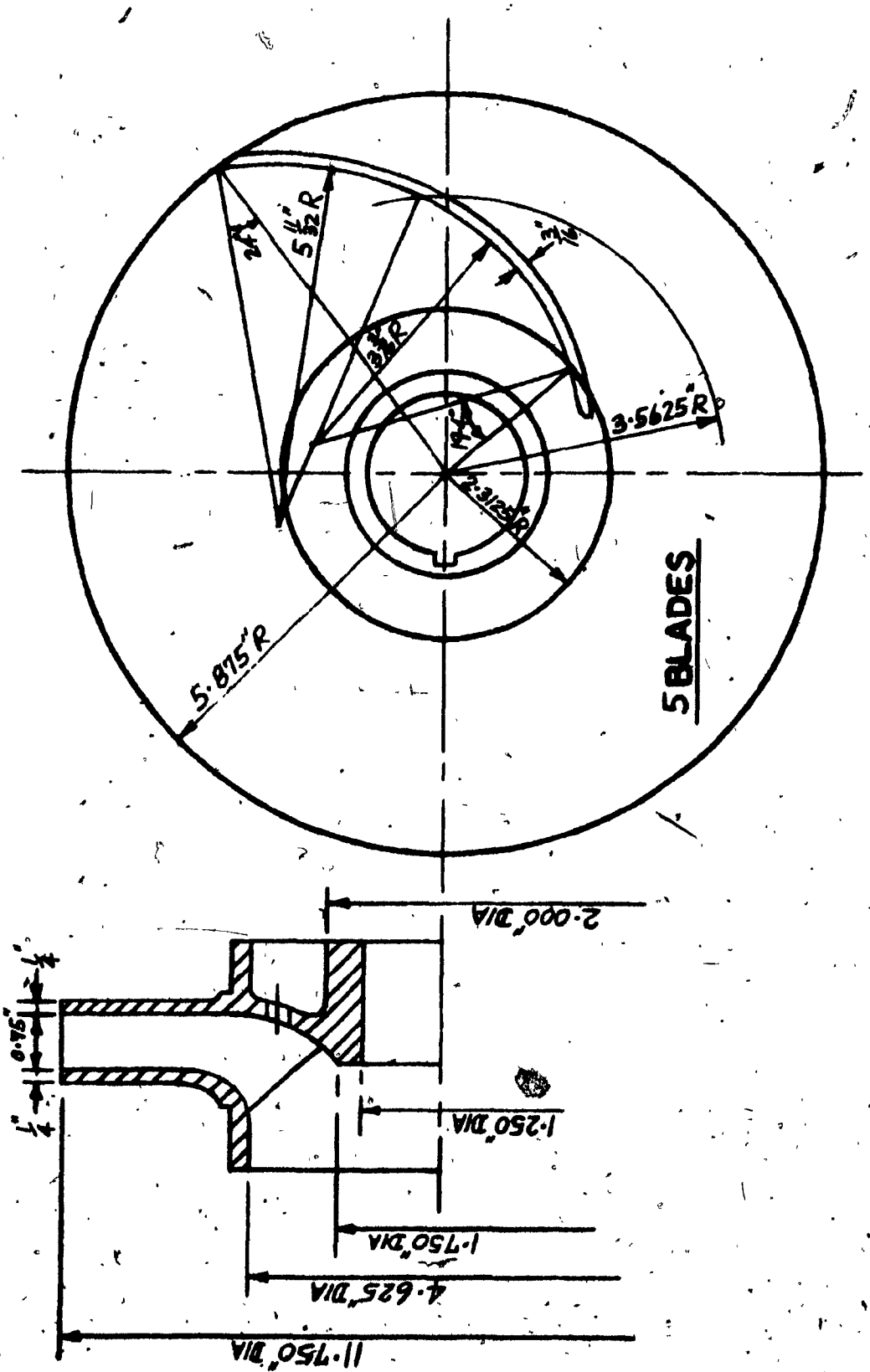

NOT TO SCALE

Figure A-3 - Impeller Drawing

Dimensions of Casing

$$\frac{C_{th}}{u_2} = 0.5 \text{ (Value read from Fig. 3.1)}$$

So, $C_{th} = 0.5\ u_2$

$= 0.5 \times 89.7$

$= 44.85$ ft/sec

From Equation (3.1):

$$A_{th} = \frac{.321\ Q}{C_{th}}$$

$$= \frac{.321 \times 500}{44.85}$$

$$= 3.58 \text{ ins}^2$$

$$A_v = \frac{\phi_v}{360} \times A_{th}$$

$$A_v = \frac{\phi_v}{360} \times 3.58$$

$$= .01\phi_v$$

Values of ϕ_v can be chosen between 0° and 360° and volute areas A_v can be determined:

ϕ_v degrees	A_v ins^2
45	0.45
90	0.9
135	1.35
180	1.8
225	2.25
270	2.7
315	3.15
360	3.6

For volute section, a rectangular shape is chosen having an area equal to $b_3 \times h$. b_3 is taken as two times the impeller discharge width. So, b_3 is equal to $2b_2$. Therefore,

$$b_3 = 2 \times 3/4$$
$$= 1\ 1/2 \text{ inches}$$

And,

$$h = \frac{A_v}{b_3}$$

A_v ins^2	h ins	h ins
0.45	0.3	5/16
0.9	0.6	19/32
1.35	0.9	7/8
1.8	1.2	1 3/16
2.25	1.5	1 1/2
2.7	1.8	1 13/16
3.15	2.1	2 3/32
3.6	2.4	2 3/8

The tongue angle ϕ_t is (Equation 3.3)

$$\phi_t = \frac{132 \log_{10} R_t/R_2}{\tan \alpha_2'}$$

Where

$$R_t = 1.05\ R_2$$
$$= 1.05 \times 5.875$$
$$= 6.16875$$

And,

$$\alpha_2' = 6.4°$$

Therefore, $$\phi_t = \frac{132 \log 6.16875/5.875}{\tan 6.4}$$

$$= 24.94°, \text{ say } 25°$$

The volute terminates in a conical diffuser. From Figure 3.5,

$$\alpha_3 = 8.2°$$

$$\tan \frac{\alpha_3}{2} = \frac{D_o - D_{th}}{2L}$$

Let D_o = 4 inches and D_{th} = 2.13 inches.

Therefore, $$L = \frac{4 - 2.13}{2 \tan \frac{8.2}{2}}$$

$$= 13.043, \text{ say } 13\ 1/16"$$

The length L seems to be long and in fact, it can be reduced by using the angles α_3 equal to 10°.

Thus, $$L = \frac{4 - 2.13}{2 \tan \frac{10}{2}} = 10.687, \text{ say } 10\ 11/16"$$

Figure A-4 represents the casing drawing.

Radial Thrust

The radial thrust is (Equation 4.1):

$$F_r = K_r\ p\ D_2\ B_2$$

In terms of head, the equation changes to

$$F_r = K_r \frac{H}{2.31} D_2\ B_2$$

The radial thrust is considered at zero flow condition since it is maximum at this point. The actual value of head developed at Q equal to zero can only be determined experimentally, but for design purpose, the

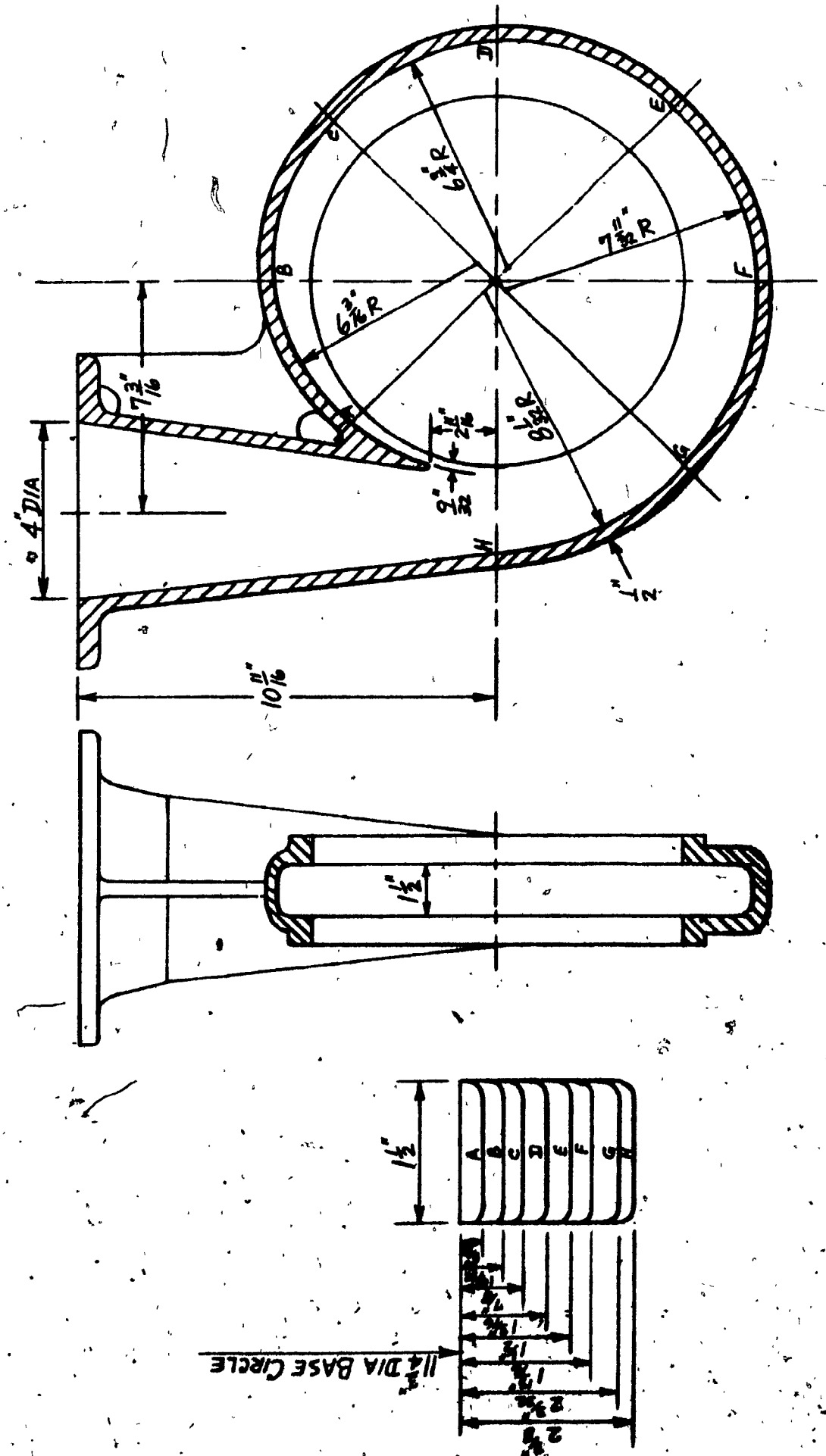

Figure A-4 - Casting Drawing

head at zero flow is taken as 1.2 times the head at design point. Therefore:

$$H_o = 1.2 \times 130$$
$$= 156 \text{ feet}$$

And, $B_2 = b_2 + (2 \times \text{thickness of shroud})$
$$= 0.75 + (2 \times 1/4)$$
$$= 1.25 \text{ inches}$$

Value of $K_r = 0.16$ (read from Figure 4.1)

Therefore, $F_r = 0.16 \times \frac{156}{2.31} \times 11.75 \times 1.25$
$$= 158.7 \text{ lb}$$

Axial Thrust

The case is of single suction overhung impeller. There are two axial forces. One is balanced by providing front and back wearing rings of equal diameters and drilling balanced holes in the impeller shroud (Fig. 4.5) whereas, the second have to be taken into consideration. If the pump operates on suction lift, the magnitude of second axial force is negligible. But if the same pump operates under suction pressure, a large amount of the axial thrust is generated. Assume a suction pressure of 100 psi, the maximum suction pressure encountered in the field. Taking shaft diameter through the stuffing box as 1 1/2", shaft area is:

$$A_s = \frac{\pi}{4} \times 1.50^2$$
$$= 1.77 \text{ ins}^2$$

Therefore, the axial force Fa is equal to the product of the shaft area through the stuffing box and the difference between the suction and

atmospheric pressure.

Therefore, $Fa_2 = (100 - 14.7) \times 1.77$

$= 151$ lbs

This force acts towards the coupling end.

Bearings

At this point, the weight of the impeller should be known. The weight of the impeller can be calculated approximately. The impeller is cast in cast iron having a specific gravity of 7.2. The density of cast iron is specific gravity times density of water at ambient temperature. Therefore density of cast iron is 449.28 pounds per ft^3. The total volume of impeller can be considered to be made up of the volume of the front shroud plus the volume of the back shroud. Hence, the volume of impeller is 0.033 ft^3. This gives an impeller weight of 14.8 pounds but to be safe, the weight will be taken as 20 pounds. The load W overhangs the two bearings:

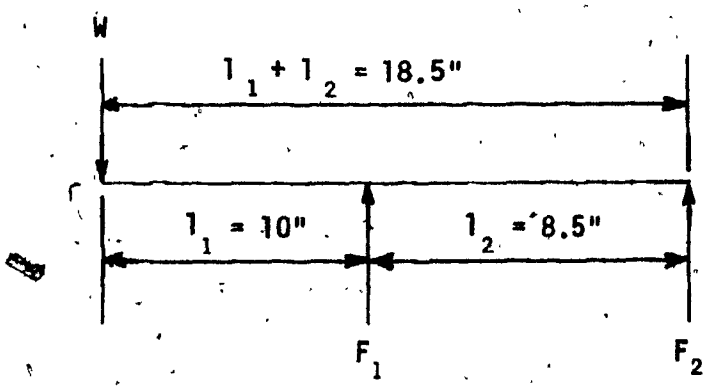

The load W is the vector sum of impeller weight plus radial thrust.

$$W = \sqrt{20^2 + 158.7^2}$$

$= 160$ pounds

Now, $$F_1 = \frac{W \times (l_1 + l_2)}{l_2}$$

$$= \frac{160 \times 18.5}{8.5}$$

$$= 348.24 \text{ lbs}$$

And, $$F_2 = \frac{W \times l_1}{l_2}$$

$$= \frac{160 \times 10}{8.5}$$

$$= 188.24 \text{ lbs}$$

The bearing at F_1 is not subjected to axial load whereas the bearing at F_2 is acted upon by axial load. Pump duty can be intermittent or continuous. The bearing life is selected as 20,000 life hours for intermittent duty [42].

Check ratio $\frac{Fa_2}{VF_2} > e$, to determine if axial load has to be considered in selecting the bearing at F_2. The rotation factor V is one for a bearing with inner rotating ring. Therefore,

$$\frac{Fa_2}{F_2} = \frac{151}{188.24}$$

$$= 0.8$$

This value of 0.8 is greater than the value of e in Table 1 and, therefore, axial load has an influence on the equivalent bearing load. The equation for calculating equivalent bearing load P is [43]:

$$P = XVF_2 + YFa_2$$

where P is equivalent bearing load, X is radial factor of bearing and y is thrust factor of bearing. Select tentatively values of X and Y from

TABLE 1

Factors V, X and Y for Radial Bearings

Bearing Type			In Relation to the Load the Inner Ring is		Single Row Bearings 1)		Double Row Bearings 2)				e
			Rotating	Stationary	$\frac{F_a}{VF_r} > e$		$\frac{F_a}{VF_r} \leq e$		$\frac{F_a}{VF_r} > e$		
			V	V	X	Y	X	Y	X	Y	
3) Radial Contact Groove Ball Bearings	4) $\frac{F_a}{C_0}$	5) $\frac{F_a}{i Z D_w^2}$									
	0.014	25				2.30				2.30	0.19
	0.028	50				1.99				1.99	0.22
	0.056	100				1.71				1.71	0.26
	0.084	150				1.55				1.55	0.28
	0.11	200	1	1.2	0.56	1.45	1	0	0.56	1.45	0.30
	0.17	300				1.31				1.31	0.34
	0.28	500				1.15				1.15	0.38
	0.42	750				1.04				1.04	0.42
	0.56	1000				1.00				1.00	0.44
20°					0.43	1.00		1.09	0.70	1.63	0.57
25°					0.41	0.87		0.92	0.67	1.44	0.68
30°			1	1.2	0.39	0.76	1	0.78	0.63	1.24	0.80
35°					0.37	0.66		0.66	0.60	1.07	0.95
40°					0.35	0.57		0.55	0.57	0.93	1.14
Self-Aligning Ball Bearings			1	1	0.40	0.4 cot α	1	0.42 cot α	0.65	0.65 cot α	1.5 tan α
Self-Aligning and Tapered Roller Bearings			1	1.2	0.40	0.4 cot α	1	0.45 cot α	0.67	0.67 cot α	1.5 tan α

SKF [44]

Table 1. Choosing X = 0.56 and Y = 2.3,

$$P = 0.56 \times 188.24 + 2.3 \times 151$$

$$= 452.7 \text{ lbs.}$$

From Table 2, after interpolation, the loading ratio $\frac{C}{P}$ equals 12.8, where C is dynamic basic capaicty of bearing.

Therefore, $C = 12.8 \times P$

$$= 12.8 \times 452.7 \text{ lbs}$$

$$= 5794.56 \text{ lbs}$$

Checking in the Table 3 for single row deep groove ball bearings, the bearing number 6210 have a dynamic capacity C of 6100 lbs and static capacity C_o of 4650 lbs. The next step is to verify whether the values of the factors X and Y are correctly chosen. Determine the value of the ratio, Fa_2/C_o. Therefore,

$$\frac{Fa_2}{C_o} = \frac{151}{4650} = 0.032$$

Values of X = 0.56 and Y = 1.95 are obtained after interpolation from Table 1. The new value of equivalent bearing load is:

$$P = 0.56 \times 188.24 + 1.95 \times 151$$

$$= 399.86 \text{ lbs}$$

The loading ratio for the selected bearing is

$$\frac{C}{P} = \frac{6100}{399.86}$$

$$= 15.3$$

This value is greater than that required (12.8) and therefore, bearing

TABLE 2

C/P Values in Relation to Speed and Life

Ball Bearings

Life Hours	Speed RPM																
	25	50	100	200	300	500	600	750	900	1000	1200	1500	1800	2400	3600	5000	10000
	Load-Ratio *C/P*																
100				1.06	1.22	1.44	1.53	1.65	1.75	1.82	1.93	2.06	2.21	2.42	2.78	3.11	3.91
500		1.14	1.44	1.82	2.06	2.47	2.62	2.82	3.00	3.11	3.30	3.56	3.78	4.16	4.76	5.31	6.69
1000	1.14	1.44	1.82	2.29	2.62	3.11	3.30	3.56	3.78	3.91	4.16	4.48	4.76	5.24	6.00	6.69	8.43
1250	1.23	1.55	1.96	2.47	2.82	3.35	3.56	3.83	4.07	4.22	4.48	4.83	5.13	5.65	6.46	7.21	9.09
1600	1.34	1.69	2.13	2.68	3.07	3.63	3.86	4.16	4.42	4.58	4.87	5.24	5.57	6.13	7.02	7.83	9.86
2000	1.44	1.82	2.29	2.88	3.30	3.91	4.16	4.48	4.76	4.93	5.24	5.65	6.00	6.60	7.56	8.43	10.6
2500	1.55	1.96	2.47	3.11	3.56	4.22	4.48	4.83	5.13	5.31	5.65	6.08	6.46	7.11	8.14	9.09	11.4
3200	1.69	2.13	2.68	3.37	3.86	4.58	4.86	5.24	5.57	5.77	6.13	6.60	7.02	7.72	8.84	9.86	12.4
4000	1.82	2.29	2.88	3.63	4.16	4.93	5.24	5.65	6.00	6.21	6.60	7.11	7.56	8.32	9.52	10.6	13.4
5000	1.96	2.47	3.11	3.91	4.48	5.31	5.65	6.08	6.46	6.69	7.11	7.66	8.14	8.96	10.3	11.4	14.4
6300	2.11	2.66	3.36	4.23	4.84	5.74	6.10	6.57	6.98	7.23	7.68	8.28	8.80	9.68	11.1	12.4	15.6
8000	2.29	2.88	3.63	4.58	5.24	6.21	6.60	7.11	7.56	7.83	8.32	8.96	9.52	10.5	12.0	13.4	16.9
10000	2.47	3.11	3.91	4.93	5.65	6.69	7.11	7.66	8.14	8.43	8.96	9.65	10.3	11.3	12.9	14.4	18.2
12500	2.66	3.35	4.22	5.31	6.08	7.21	7.66	8.25	8.77	9.09	9.65	10.4	11.1	12.2	13.9	15.5	19.6
16000	2.88	3.63	4.58	5.77	6.60	7.83	8.32	8.96	9.52	9.86	10.5	11.3	12.0	13.2	15.1	16.8	21.3
20000	3.11	3.91	4.93	6.21	7.11	8.43	8.96	9.65	10.3	10.6	11.3	12.2	12.9	14.2	16.2	18.2	22.9
25000	3.35	4.22	5.31	6.69	7.66	9.09	9.65	10.4	11.1	11.4	12.2	13.1	13.9	15.3	17.5	19.6	24.7
32000	3.63	4.58	5.77	7.27	8.32	9.86	10.5	11.3	12.0	12.4	13.2	14.2	15.1	16.6	19.0	21.3	26.8
40000	3.91	4.93	6.21	7.83	8.96	10.6	11.3	12.2	12.9	13.4	14.2	15.3	16.3	17.9	20.5	22.9	28.8
50000	4.22	5.31	6.69	8.43	9.65	11.4	12.2	13.1	13.9	14.4	15.3	16.5	17.5	19.3	22.1	24.7	31.1
63000	4.55	5.74	7.23	9.11	10.4	12.4	13.1	14.2	15.0	15.6	16.6	17.8	18.9	20.9	23.9	26.6	
80000	4.93	6.21	7.83	9.86	11.3	13.4	14.2	15.3	16.3	16.9	17.9	19.3	20.5	22.6	25.9	28.8	
100000	5.31	6.69	8.43	10.6	12.2	14.4	15.3	16.5	17.5	18.2	19.3	20.8	22.1	24.3	27.8	31.1	
200000	6.69	8.43	10.6	13.4	15.3	18.2	19.3	20.8	22.1	22.9	24.3	26.2	27.8	30.7			

SKF [45]

SINGLE ROW DEEP GROOVE BALL BEARINGS

Metric Dimension Series 02

Bearing Series 62	Bearing Series 62-Z	Bearing Series 62-2Z	Bearing Series 62-RS	Bearing Series 62-2RS

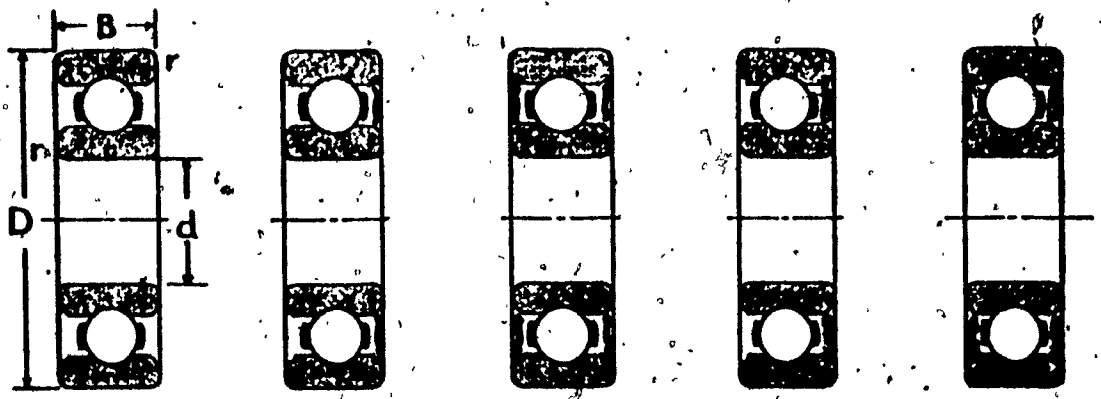

Open — One Shield — Two Shields — One Rod Seal — Two Rod Seals

TABLE 3

Bearing Dimensions

Bearing No.	d		D		B		r [1]	Basic capacity, lb.		Max.[2] permissible speed r.p.m.
	mm.	in.	mm.	in.	mm.	in.	mm.	Static C_0	Dynamic C	
6200	10	0.3937	30	1.1811	9	0.3543	1	430	800	20000
01	12	0.4724	32	1.2598	10	0.3937	1	465	1150	19000
02	15	0.5906	35	1.3780	11	0.4331	1	780	1220	18000
6201	12	0.4724	32	1.2598	10	0.3937	1	585	1040	18000
01	16	0.6299	37	1.4567	12	0.4724	1.5	1020	1600	17000
02	17	0.6693	40	1.5748	12	0.4724	1.5	1430	2200	16000
03	20	0.7874	47	1.8504	14	0.5512	1.5	1560	2600	13000
04	25	0.9843	52	2.0472	15	0.5906	2	2200	3250	12000
6202	15	0.5906	35	1.3780	11	0.4331	1	780	1220	18000
01	18	0.7087	42	1.6535	12	0.4724	1.5	1140	1800	17000
02	20	0.7874	47	1.8504	14	0.5512	1.5	1430	2280	16000
03	25	0.9843	52	2.0472	15	0.5906	2	2200	3250	13000
04	30	1.1811	62	2.4409	16	0.6299	2	2700	4000	12000
6203	17	0.6693	40	1.5748	12	0.4724	1	1020	1600	17000
01	20	0.7874	47	1.8504	14	0.5512	1.5	1430	2200	16000
02	25	0.9843	52	2.0472	15	0.5906	2	2200	3250	13000
03	30	1.1811	62	2.4409	16	0.6299	2	2700	4000	12000
04	35	1.3780	72	2.8346	17	0.6693	2	3450	4650	10000
05	40	1.5748	80	3.1496	18	0.7087	2	3450	5000	10000
6204	20	0.7874	47	1.8504	14	0.5512	1.5	1430	2280	16000
01	25	0.9843	52	2.0472	15	0.5906	2	2200	3250	13000
02	30	1.1811	62	2.4409	16	0.6299	2	2700	4000	12000
03	35	1.3780	72	2.8346	17	0.6693	2	3450	4650	10000
04	40	1.5748	80	3.1496	18	0.7087	2	3450	5000	10000
05	45	1.7717	85	3.3465	19	0.7480	2	4000	5400	9000
6205	25	0.9843	52	2.0472	15	0.5906	2	2200	3250	13000
01	30	1.1811	62	2.4409	16	0.6299	2	2700	4000	12000
02	35	1.3780	72	2.8346	17	0.6693	2	3450	4650	10000
03	40	1.5748	80	3.1496	18	0.7087	2	3450	5000	10000
04	45	1.7717	85	3.3465	19	0.7480	2	4000	5400	9000
05	50	1.9685	90	3.5433	20	0.7874	2	4550	6100	8500
06	55	2.1654	100	3.9370	21	0.8268	2.5	5700	7800	8000
6206	30	1.1811	62	2.4409	16	0.6299	2	2700	4000	12000
01	32	1.2598	72	2.8346	17	0.6693	2	3450	4650	10000
02	35	1.3780	72	2.8346	17	0.6693	2	3450	4650	10000
03	40	1.5748	80	3.1496	18	0.7087	2	3450	5000	10000
04	45	1.7717	85	3.3465	19	0.7480	2	4000	5400	9000
05	50	1.9685	90	3.5433	20	0.7874	2	4550	6100	8500
06	55	2.1654	100	3.9370	21	0.8268	2.5	5700	7800	8000
6207	35	1.3780	72	2.8346	17	0.6693	2	3450	4650	10000
01	40	1.5748	80	3.1496	18	0.7087	2	3450	5000	10000
02	45	1.7717	85	3.3465	19	0.7480	2	4000	5400	9000
03	50	1.9685	90	3.5433	20	0.7874	2	4550	6100	8500
04	55	2.1654	100	3.9370	21	0.8268	2.5	5700	7800	8000
05	60	2.3622	110	4.3307	22	0.8661	2.5	7100	9300	6700
06	65	2.5591	120	4.7244	23	0.9055	2.5	7800	10200	6300
07	70	2.7559	125	4.9213	24	0.9449	2.5	8450	11000	5600
6208	40	1.5748	80	3.1496	18	0.7087	2	3450	5000	10000
01	45	1.7717	85	3.3465	19	0.7480	2	4000	5400	9000
02	50	1.9685	90	3.5433	20	0.7874	2	4550	6100	8500
03	55	2.1654	100	3.9370	21	0.8268	2.5	5700	7800	8000
04	60	2.3622	110	4.3307	22	0.8661	2.5	7100	9300	6700
05	65	2.5591	120	4.7244	23	0.9055	2.5	7800	10200	6300
06	70	2.7559	125	4.9213	24	0.9449	2.5	8450	11000	5600
6209	45	1.7717	85	3.3465	19	0.7480	2	4000	5400	9000
01	50	1.9685	90	3.5433	20	0.7874	2	4550	6100	8500
02	55	2.1654	100	3.9370	21	0.8268	2.5	5700	7800	8000
03	60	2.3622	110	4.3307	22	0.8661	2.5	7100	9300	6700
04	65	2.5591	120	4.7244	23	0.9055	2.5	7800	10200	6300
05	70	2.7559	125	4.9213	24	0.9449	2.5	8450	11000	5600
06	75	2.9528	130	5.1181	25	0.9843	2.5	9300	11400	5300
6210	50	1.9685	90	3.5433	20	0.7874	2	4550	6100	8500
01	55	2.1654	100	3.9370	21	0.8268	2.5	5700	7800	8000
02	60	2.3622	110	4.3307	22	0.8661	2.5	7100	9300	6700
03	65	2.5591	120	4.7244	23	0.9055	2.5	7800	10200	6300
04	70	2.7559	125	4.9213	24	0.9449	2.5	8450	11000	5600
05	75	2.9528	130	5.1181	25	0.9843	2.5	9300	11400	5300
06	80	3.1496	140	5.5118	26	1.0236	3	10000	12500	5000
07	85	3.3465	150	5.9055	28	1.1024	3	11600	14300	4800
6211	55	2.1654	100	3.9370	21	0.8268	2.5	5700	7800	8000
01	60	2.3622	110	4.3307	22	0.8661	2.5	7100	9300	6700
02	65	2.5591	120	4.7244	23	0.9055	2.5	7800	10200	6300
03	70	2.7559	125	4.9213	24	0.9449	2.5	8450	11000	5600
04	75	2.9528	130	5.1181	25	0.9843	2.5	9300	11400	5300
05	80	3.1496	140	5.5118	26	1.0236	3	10000	12500	5000
06	85	3.3465	150	5.9055	28	1.1024	3	11600	14300	4800
07	90	3.5433	160	6.2992	30	1.1811	3	13200	16400	4500
6212	60	2.3622	110	4.3307	22	0.8661	2.5	7100	9300	6700
01	65	2.5591	120	4.7244	23	0.9055	2.5	7800	10200	6300
02	70	2.7559	125	4.9213	24	0.9449	2.5	8450	11000	5600
03	75	2.9528	130	5.1181	25	0.9843	2.5	9300	11400	5300
04	80	3.1496	140	5.5118	26	1.0236	3	10000	12500	5000
05	85	3.3465	150	5.9055	28	1.1024	3	11600	14300	4800
06	90	3.5433	160	6.2992	30	1.1811	3	13200	16400	4500
6213	65	2.5591	120	4.7244	23	0.9055	2.5	7800	10200	6300
01	70	2.7559	125	4.9213	24	0.9449	2.5	8450	11000	5600
02	75	2.9528	130	5.1181	25	0.9843	2.5	9300	11400	5300
03	80	3.1496	140	5.5118	26	1.0236	3	10000	12500	5000
04	85	3.3465	150	5.9055	28	1.1024	3	11600	14300	4800
05	90	3.5433	160	6.2992	30	1.1811	3	13200	16400	4500
06	95	3.7402	170	6.6929	32	1.2598	3.5	15600	19300	4300
07	100	3.9370	180	7.0866	34	1.3386	3.5	16600	21200	3900
6214	70	2.7559	125	4.9213	24	0.9449	2.5	8450	11000	5600
01	75	2.9528	130	5.1181	25	0.9843	2.5	9300	11400	5300
02	80	3.1496	140	5.5118	26	1.0236	3	10000	12500	5000
03	85	3.3465	150	5.9055	28	1.1024	3	11600	14300	4800
04	90	3.5433	160	6.2992	30	1.1811	3	13200	16400	4500
05	95	3.7402	170	6.6929	32	1.2598	3.5	15600	19300	4300
06	100	3.9370	180	7.0866	34	1.3386	3.5	16600	21200	3900
6215	75	2.9528	130	5.1181	25	0.9843	2.5	9300	11400	5300
01	80	3.1496	140	5.5118	26	1.0236	3	10000	12500	5000
02	85	3.3465	150	5.9055	28	1.1024	3	11600	14300	4800
03	90	3.5433	160	6.2992	30	1.1811	3	13200	16400	4500
04	95	3.7402	170	6.6929	32	1.2598	3.5	15600	19300	4300
05	100	3.9370	180	7.0866	34	1.3386	3.5	16600	21200	3900
6216	80	3.1496	140	5.5118	26	1.0236	3	10000	12500	5000
01	85	3.3465	150	5.9055	28	1.1024	3	11600	14300	4800
02	90	3.5433	160	6.2992	30	1.1811	3	13200	16400	4500
03	95	3.7402	170	6.6929	32	1.2598	3.5	15600	19300	4300
04	100	3.9370	180	7.0866	34	1.3386	3.5	16600	21200	3900
6217	85	3.3465	150	5.9055	28	1.1024	3	11600	14300	4800
01	90	3.5433	160	6.2992	30	1.1811	3	13200	16400	4500
02	95	3.7402	170	6.6929	32	1.2598	3.5	15600	19300	4300
03	100	3.9370	180	7.0866	34	1.3386	3.5	16600	21200	3900
6218	90	3.5433	160	6.2992	30	1.1811	3	13200	16400	4500
01	95	3.7402	170	6.6929	32	1.2598	3.5	15600	19300	4300
02	100	3.9370	180	7.0866	34	1.3386	3.5	16600	21200	3900
6219	95	3.7402	170	6.6929	32	1.2598	3.5	15600	19300	4300
01	100	3.9370	180	7.0866	34	1.3386	3.5	16600	21200	3900
6220	100	3.9370	180	7.0866	34	1.3386	3.5	16600	21200	3900
6221	105	4.1339	190	7.4803	36	1.4173	3.5	20800	27000	3600
22	110	4.3307	200	7.8740	38	1.4961	3.5	22800	31500	3400
24	120	4.7244	215	8.4646	40	1.5748	3.5	26000	36000	3200
6222	110	4.3307	200	7.8740	38	1.4961	3.5	22800	31500	3400
24	120	4.7244	215	8.4646	40	1.5748	3.5	26000	36000	3200
6224	120	4.7244	215	8.4646	40	1.5748	4	26000	36000	3200
6226	130	5.1181	230	9.0551	40	1.5748	4	27500	37000	3000
28	140	5.5118	250	9.8425	42	1.6535	4	30500	42500	2800
30	150	5.9055	270	10.6299	45	1.7717	4	31500	44000	2600
6232	160	6.2992	290	11.4173	48	1.8898	4	34000	51000	2400
34	170	6.6929	310	12.2047	52	2.0472	5	41500	58500	2200
36	180	7.0866	320	12.5984	52	2.0472	5	43000	61000	2000
6238	190	7.4803	340	13.3858	55	2.1654	5	47500	66000	1900
40	200	7.8740	360	14.1732	58	2.2835	5	49500	69500	1800

6210 is suitable. Bearing at F_1 is selected on the basis of radial load only.

$$P = F_1 = 348.24$$

The loading ratio is the same as before. Therefore,

$$C = 12.8 \times P$$

$$= 12.8 \times 348.24$$

$$= 4457.5 \text{ lbs.}$$

From Table 3, bearing number 6208 have a dynamic capaicty C of 5000 lbs, which is greater than what is required (4457.5). So, bearing 6208 will do the job.

Critical Speed

The shaft will be checked for critical speed. The shaft can be represented, as shown below, with various loads and forces acting on it.

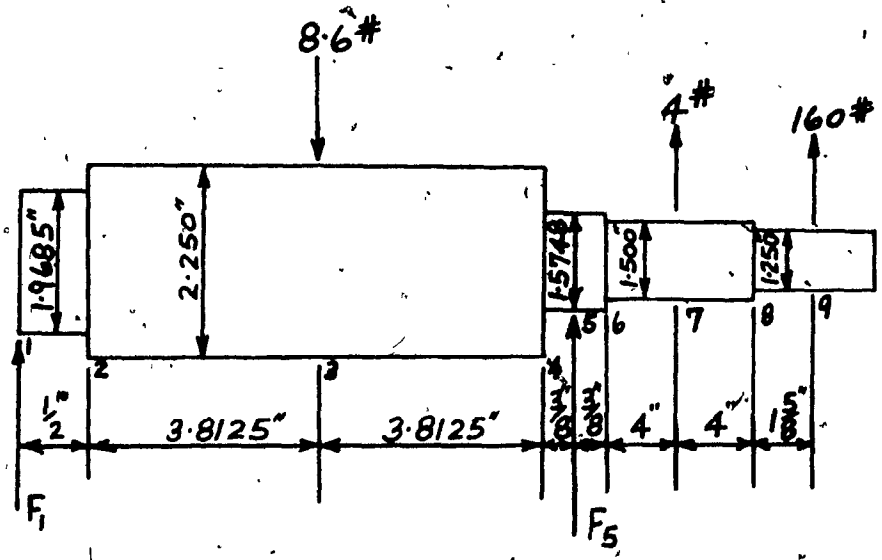

8.6 and 4 are the shaft weight in pounds. 160 pounds is the vector sum of impeller weight and radial thrust.

F_1 and F_5 are the reactions on the bearings that are to be evaluated. Upward forces are considered positive.

Taking moments,

$$F_1 \times 8.5 = 8.6 \times 4.1875 + 4 \times 4.375 + 160 \times 10$$

$$F_1 = 194.53 \text{ lbs}$$

$$F_5 \times 8.5 + 4 \times 12.875 + 160 \times 18.5 = 8.6 \times 4.3125$$

$$F_5 = -.350 \text{ lbs}$$

The procedure for calculating the shaft deflection is described and then the calculations are tabulated.

Step-by-Step Procedure for Finding Shaft Deflection [47]

1. Divide shaft into lengths with intervals beginning at each force and change of section.
2. Label the ends of intervals with station numbers beginning at the left-hand reaction.
3. List station numbers on alternate lines in the first column of calculation sheet.
4. List reactions and forces in column 2 on the same lines as the station numbers at which they occur.
5. Calculate the vertical shear at each station by summing values in column 2. Tabulate each shear value in column 3, one station below the station for which is calculated. The last shear force should be numerically equal to, but opposite in sigh to the last force listed in column 2.
6. In column 4, on the same line as the station number, list the distance to preceeding station.
7. Calculate bending moments at each station and list the values in column 5. Value at the first station is zero. Values at succeeding

stations are obtained by summing products of Column 3 and Δx (column 4).

8. Calculate the moment of inertia I in bending for each interval. Place the I values in column 6 on the line between two stations at which the interval begins and ends.

9. Multiply each I value by modulus of elasticity E and insert the EI values in column 7 on same lines as corresponding I values. Here value of E equals to 30×10^6 psi.

10. Divide each bending-moment value in column 5 by the EI values in column 7 which precedes and follow it. List these values in column 8.

11. Obtain the average M/EI value for each interval by averaging the values on the line on which station is listed and the following line. List the average values on the lines between stations in column 9.

12. Calculate the slope values in column 10 starting with station 1. Succeeding values are obtained by summing products of $(M/EI)_{avg}$ from column 9 and the Δx value on the next lower line of column 4. These values are listed on the same lines as the stations.

13. Average the slope values in column 10 at the beginning and end of each interval. These values are listed on lines between stations in column 11.

14. Obtain the deflection increment values in column 12 by multiplying the average slope value in column 11 and the Δx value from the next lower line in column 4.

15. Sum the deflection increments of column 12, only those from stations 1 and 5 are included. Thus, Σy equals 446.59. The sign is changed. So the integration constant is $\frac{-446.59}{8.5} = -52.54$ mu in per inch,

where 8.5 is the distance between the reactions. This constant is multiplied by the Δx values in column 4 to obtain the integration constant for each interval. These products are listed on the same lines as the average slope and deflection increments.

16. In column 14, zeros are placed opposite the stations at which reactions occur. Next, the deflection increment and integration constant values downward from the left-hand reaction are summed together. Finally, the deflection values are put on the same lines as the station numbers.

W lbs	y ins	W Y lb-in	W Y^2 lb-in^2
- 8.6	-134.23×10^{-6}	1154.38×10^{-6}	0.155×10^{-6}
4.0	1694.41×10^{-6}	6777.64×10^{-6}	11.484×10^{-6}
160.0	6142.4×10^{-6}	9827.84×10^{-6}	6036.6×10^{-6}

Σ WY = 0.991

ΣWY^2 = 0.006

Now, $$N_c = 187.5 \left[\frac{\Sigma WY}{\Sigma WY^2}\right]^{1/2}$$

$$= 187.5 \left[\frac{0.991}{.006}\right]^{1/2}$$

$$= 2400 \text{ rpm}$$

So, the critical speed is greater than the operating speed (1750 rpm) and hence, the shaft is safely designed.

TABLE 4

Shaft Deflection Calculation

1 Station Number From Left	2 Force or Reaction lbs	3 Shear at Preceding Stations lbs	4 Distance Between Stations Δx-ins	5 Bending Moment M lb-ins	6 Moment of Inertia I-ins^4	7 EI 10^6 lb-ins	8 M/EI $\left(\frac{1}{\text{mu-ins}}\right)$	9 Average Column 8 $\left(\frac{1}{\text{mu-ins}}\right)$	10 Slope mu Radian	11 Average Slope mu Radian	12 Deflection Increment mu-ins	13 Integration Constant mu-ins	14 Calculated Deflection y mu-ins	1 Station Number, From Left
1	194.5			0			0		0				0.00	1
					.74	22.2	4.38	2.19		0.55	.275	- 26.27		
2		194.5	0.5	97.25			2.57		1.1				- 25.99	2
					1.26	37.8	22.19	12.38		24.15	92.07	-200.31		
3	- 8.6	194.5	3.8125	838.8			22.19		47.20				-134.23	3
					1.26	37.8	40.94	31.57		83.78	319.41	-200.31		
4		185.9	3.8125	1547.5			171.94		120.36				- 15.13	4
					.30	9.0	176.69	174.32		92.87	34.83	- 19.70		
5	- 350	185.9	.375	1617.2			176.69		65.37				0.00	5
					.30	9.0	172.86	174.78		65.46	24.55	19.70		
6		- 164.1	.375	1555.7			207.42		65.54				44.25	6
					.25	7.5	119.91	163.67		360.11	1440.44	210.16		
7	4	- 164.1	4	899.3			119.91		654.68				1694.41	7
					.25	7.5	34.52	77.22		963.56	3854.24	210.16		
8		- 160.1	4	258.9			71.92		308.88				5758.81	8
					.12	3.6	- .36	35.78		183.51	298.20	85.38		
9	160	- 160.1	1.625	- 1.3					58.14				6142.4	9